Interaction Notes

Note 192

31 August 1974

EFFECTS OF BRAID RESISTANCE AND WEATHERPROOFING JACKETS ON COAXIAL CABLE SHIELDING

K. F. Casey

Department of Electrical Engineering
Kansas State University/Manhattan, Kansas

ABSTRACT

The effects of finite conductivity in the shield conductors and of the presence of dielectric weatherproofing jackets on coaxial cable shielding are investigated by considering three coaxial-cable shield models. The first of these is a bidirectionally conducting shell; the second is a concentric pair of counterwound unidirectionally conducting shells; and the third is a pair of M-filar counterwound filamentary helices with a (possibly lossy) dielectric jacket. For each model, the transmission-line parameters are determined. Comparison of the results for the first two models indicates the importance of the woven shield structure, in that for the first model, the coupling impedance decreases exponentially as the shield thickness increases; and for the second, the decrease is generally only algebraic. The results for the third model indicate that a dielectric jacket tends to reduce the electric-field coupling to the interior of the cable, and that the finite resistance of the shield conductors for this case is not of great importance as long as it is small.

This study was performed under subcontract to

The Dikewood Corporation
1009 Bradbury Drive
University Research Park
Albuquerque, New Mexico 87106

and has been fully supported by the Defense Nuclear Agency (DNA) under

DNA Subtask EB088
EMP Interaction and Coupling
DNA Work Unit 32
Coaxial Cables

CONTENTS

ILLUSTRATIONS

SECTION I

INTRODUCTION

The topic addressed in this report is the determination of the effects of finite braid resistance and/or dielectric weatherproofing jackets on coaxial-cable shielding. To this end, we have considered three specific shield models and have determined the transmission-line parameters for a coaxial cable with each type of shield.

Typically, coaxial-cable shields are constructed of many fine copper wires arranged in bands, these bands being woven together in a herringbone pattern. At the positions where the bands of wires overlap, there occur small diamond-shaped apertures in the shield. Thus there exist two principal mechanisms by which electromagnetic energy can be coupled from the exterior to the interior of a cable: diffusion across the shield wires and penetration of the apertures. The calculation of the diffused field is complicated by the fact that the shield is neither isotropic nor homogeneous, owing to its braided construction; and the aperture-penetration calculations are difficult because the shield apertures are not of a shape for which exact solutions are known. Additionally, the effects of mutual coupling are difficult to take into account.

If the shield wires were perfectly conducting and if there were no apertures in the shield, the shield would be perfect in the sense that no energy could penetrate into the cable interior from the exterior. The finite braid resistance of an actual shield without apertures is part and parcel of the imperfect shielding inherent in such a shield, since the finite braid resistance results from the finite skin depth, which permits diffusion to take place. Furthermore, for a shield without apertures (optical coverage = 1), an external dielectric jacket surrounding the cable will have no effect on the cable parameters, and thus on the shielding effectiveness, so long as the jacket is electrically thin. This is so because the jacket will not carry any appreciable current, and thus will not "help" the conducting shield. Additionally, if there are no apertures in the shield, electric field lines in the interior of the cable will terminate on the inner surface of the shield and not penetrate the jacket.

If, on the other hand, the shield is "sparse," that is, if its optical coverage is much less than unity, the finite resistance of the shield wires would not be expected to be very important, since the primary coupling mechanism in such a cable would be through aperture penetration. In this case, an outer dielectric jacket on the cable would be expected to have a significant effect on the cable parameters (at least the shunt admittance and current-source terms) since the electric field of the cable interior would penetrate the jacket.

The three problems considered in this report are intended to illustrate these notions. In the first and second shield models, there are no shield apertures; and the third shield model is sparse, and includes a dielectric jacket.

In Section II we review the basic transmission-line theory and indicate how the cable parameters are obtained from the plane-wave scattering problem. In Section III, we investigate the shield model comprising a lossy bidirectionally conducting shell; in Section IV, we consider two concentric lossy unidirectionally conducting shells as a shield model; in Section V, a sparse filamentary shield with a possibly lossy dielectric jacket is considered. The results are summarized in Section VI.

SECTION II

GENERAL CONSIDERATIONS

We shall assume (and suppress) the time dependence $\exp(j\omega t)$ for all field quantities, currents, and voltages throughout this report. Under this assumption, the transmission-line equations are

$$\frac{dV}{dz} = -ZI - Z_s I_t \tag{1a}$$

$$\frac{dI}{dz} = -YI + j\omega\Gamma_s Q_t \tag{1b}$$

in which z is the coordinate along the cable axis and where I and V denote the line voltage and current respectively. For the coaxial cables to be considered here, I is the current on the center conductor, taken to be positive in the +z-direction; and V is the potential of the center conductor with respect to the shield. Z and Y denote respectively the series impedance per unit length and the shunt admittance per unit length of the cable; and Z_s and Γ_s are respectively the transfer impedance per unit length and the (dimensionless) capacitive coupling coefficient per unit length. I_t is the total current and Q_t is the total charge per unit length on the cable.

For a lossless structure, the cable parameters Z, Y, Z_s, and Γ_s are related to the cable parameters L, C, L_s, and S_s used by Latham (ref. 1) as follows:

$$Z = j\omega L \tag{2a}$$

$$Y = j\omega C \tag{2b}$$

$$Z_s = j\omega L_s \tag{2c}$$

$$\Gamma_s = CS_s \tag{2d}$$

in which L and C are respectively the series inductance and shunt capacitance per unit length; L_s is the inductive coupling coefficient per unit length;

and S_s is the mutual susceptance per unit length. L and C are sometimes conveniently written in the forms

$$L = L_c - L_s \tag{3a}$$

$$C = \frac{1}{S_c - S_s} \tag{3b}$$

where, if the shield is confined to an electrically thin cylindrical shell region around $\rho = \rho_1$, L_c and S_c are given by

$$L_c = \frac{\mu_1}{2\pi} \ln \frac{\rho_1}{a} \tag{4a}$$

$$S_c = \frac{1}{2\pi\varepsilon_1} \ln \frac{\rho_1}{a} \tag{4b}$$

The radius of the center conductor is denoted by "a" and μ_1 and ε_1 are the permeability and permittivity of the (assumed homogeneous) medium filling the region $a \leq \rho \leq \rho_1$.

If the cable is axially uniform (or if it has a periodic shield structure whose period is much less than the axial wavelength), and if the excitation is assumed to have exponential form in the axial direction, the currents, voltage, and charge on the cable will all vary as $\exp(-j\beta_o z)$. Thus the transmission-line equations (1) become

$$-j\beta_o \hat{V} = -Z\hat{I} - Z_s \hat{I}_t \tag{5a}$$

$$-j\beta_o \hat{I} = -Y\hat{V} + j\omega\Gamma_s \hat{Q}_t \tag{5b}$$

in which $V(z) = \hat{V}\exp(-j\beta_o z)$, etc. Furthermore, it is easy to show that $\hat{Q}_t = (\beta_o/\omega)\ \hat{I}_t$, so the current-change equation (5b) may be written in the form

$$-j\beta_o \hat{I} = -Y\hat{V} + j\beta_o \Gamma_s \hat{I}_t \tag{5c}$$

The transmission-line parameters may be obtained if $\hat{I}/\hat{I}_t$ and $\hat{V}/\hat{I}_t$ are known as functions of β_o. If we define

$$\frac{\hat{I}}{\hat{I}_t} = r(\beta_o) \tag{6a}$$

$$\frac{\hat{V}}{\hat{I}_t} = \beta_o s(\beta_o) \tag{6b}$$

it is easy to show that for $\beta_o \neq 0$,

$$Z = \frac{j\beta_o^2 s(\beta_o)}{r(\beta_o) - r(0)} \tag{7a}$$

$$Z_s = -r(0)Z \tag{7b}$$

$$Y = \frac{j[r(\beta_o) - r(0)]}{s(0) - s(\beta_o)} \tag{7c}$$

$$\Gamma_s = \frac{r(0)s(\beta_o) - r(\beta_o)s(0)}{s(0) - s(\beta_o)} \tag{7d}$$

The functions $r(\beta_o)$ and $s(\beta_o)$ are obtained from the solution of the boundary-value problem of plane-wave scattering by the particular coaxial cable model under consideration, in the low-frequency limit; if the illuminating plane wave is incident at an angle θ with respect to the cable axis, then $\beta_o = -k_o\cos\theta$, where $k_o^2 = \omega^2\mu_o\varepsilon_o$. We assume that the medium exterior to the cable is free space (ε_o, μ_o); and we shall also assume that all dielectrics occurring in the various models are nonmagnetic ($\mu \approx \mu_o$). The dielectric filling the region between the center conductor, of radius a, and the inner surface of the shield, at $\rho = \rho_1$, is lossless and has permittivity ε_1. If the cable has a dielectric jacket surrounding the shield, its (possibly complex) permittivity is denoted ε_2; and the outer radius of the cable will be $\rho = \rho_o$.

The electromagnetic field is conveniently expressed in terms of two solutions Ψ and Φ of the scalar Helmholtz equation as follows:

$$\bar{E} = -\nabla \times \Phi\bar{a}_z + \frac{1}{j\omega\varepsilon} \nabla \times \nabla \times \Psi\bar{a}_z \tag{8a}$$

$$\bar{H} = \nabla \times \Psi\bar{a}_z + \frac{1}{j\omega\mu} \nabla \times \nabla \times \Phi\bar{a}_z \tag{8b}$$

If the cable structure is uniform in ϕ and z, then only the axially symmetric TM_z portion of the field is important in the region $a \leq \rho \leq \rho_1$, since it is only this part of the field which gives rise to axial currents on the structure. Thus, denoting the axially symmetric part of Ψ by Ψ_o, we have

$$\hat{V} = \frac{-\beta_o}{\omega\varepsilon_1} \hat{\Psi}_o \ (\rho_1) \tag{9a}$$

$$\hat{I} = -2\pi a \left. \frac{d\hat{\Psi}_o}{d\rho} \right|_{\rho=a} \tag{9b}$$

where

$$\hat{\Psi}_o = K[J_o(\gamma_1\rho)\ Y_o(\gamma_1 a) - J_o(\gamma_1 a)\ Y_o(\gamma_1\rho)] \tag{10}$$

with K a constant and $\gamma_1^2 = k_1^2 - \beta_o^2$, $k_1^2 = \omega^2\mu_o\varepsilon_1$. In the low-frequency limit, we find

$$\hat{V} = \frac{2\beta_o K}{\pi\omega\varepsilon_1} \ell n \frac{\rho_1}{a} \tag{11a}$$

$$\hat{I} = 4K \tag{11b}$$

As a consequence,

$$s(\beta_o) = \frac{1}{2\pi\omega\varepsilon_1} \ell n \frac{\rho_1}{a} r(\beta_o) \tag{12}$$

and therefore, choosing $\beta_o = k_1$, we have from Eq. (7)

$$Z = \frac{j\omega\mu_o}{2\pi} \ln \frac{\rho_1}{a} \frac{r(k_1)}{r(k_1) - r(0)} \tag{13a}$$

$$Z_s = -r(0)Z \tag{13b}$$

$$Y = \frac{2\pi j\omega\varepsilon_1}{\ln \frac{\rho_1}{a}} \tag{14a}$$

$$\Gamma_s = 0 \tag{14b}$$

Thus it is evident that for such structures, only Z and Z_s depend upon the specific shield model chosen. This will be the case for the first two models we shall consider, but not for the third, in which the assumption of azimuthal and axial shield uniformity is relaxed.

Finally, we point out that the total current $\hat{I}_t$ on the cylindrical cable structure is given, in the low-frequency limit, by

$$\hat{I}_t = \frac{4E_o}{\eta_o \gamma_o H_o^{(2)}(\gamma_o\rho_o)} \tag{15}$$

where $\eta_o = \sqrt{\mu_o/\varepsilon_o}$ and $\gamma_o^2 = k_o^2 - \beta_o^2$. E_o denotes the electric field amplitude in the incident wave, which is assumed to be polarized TM_z. This result applies to any circular-cylindrical cable model whose outer radius is ρ_o. We shall now investigate some specific shield models.

SECTION III

SHIELD MODEL A: A BIDIRECTIONALLY CONDUCTING SHELL

The shield model we shall consider first is a physically thin (but not necessarily electrically thin) cylindrical shell with a bidirectional conduction characteristic. Such a shell is a simple model for a braid shield, which has preferred conduction directions by virtue of its woven construction. We neglect consideration of the effects of the shield apertures.

Consider a material having two preferred directions of conduction, each making an angle ψ with respect to the z-direction as shown in Figure 1. In each preferred direction, let the conductivity be denoted σ_{11}; across each preferred direction, the conductivity is σ_1. Then denoting by $\bar{E}_{11}^{(1,2)}$ and $\bar{E}_1^{(1,2)}$ the components of the electric field parallel and perpendicular to each preferred direction, we have for the current density $\bar{J}$:

$$\bar{J} = \sigma_{11}(\bar{E}_{11}^{(1)} + \bar{E}_{11}^{(2)}) + \sigma_1(\bar{E}_1^{(1)} + \bar{E}_1^{(2)}) \tag{16}$$

or

$$\bar{J} = \sigma_\phi E_\phi \bar{a}_\phi + \sigma_z E_z \bar{a}_z \tag{17}$$

where

$$\sigma_\phi = 2\sigma_{11}(\sin^2\psi + \frac{\sigma_1}{\sigma_{11}} \cos^2\psi) \tag{18a}$$

$$\sigma_z = 2\sigma_{11}(\cos^2\psi + \frac{\sigma_1}{\sigma_{11}} \sin^2\psi) \tag{18b}$$

Now if it is assumed that the physical thickness d of the shield layer is much less than its inner radius ρ_1, we may readily obtain the matrix boundary conditions connecting the tangential components of $\bar{E}$ and $\bar{H}$ across the shield:

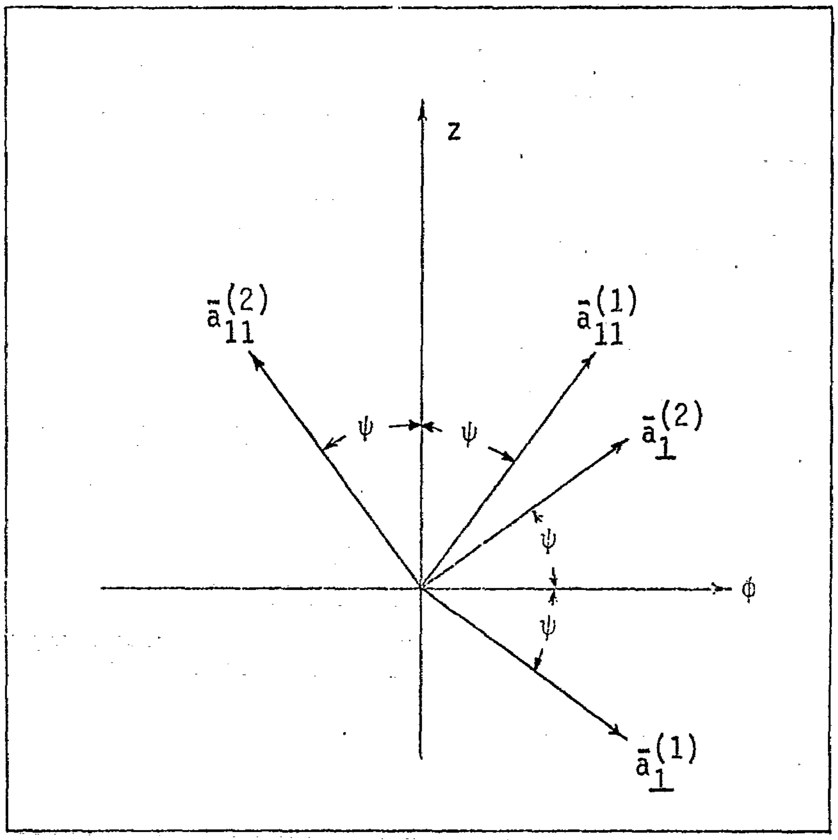

Fig. 1. Conduction directions for a bidirectionally-conducting medium.

$$\begin{bmatrix} E_z \\ \\ H_\phi \end{bmatrix}_{\rho=\rho_1+d} = \begin{bmatrix} \cosh \tau_z d & \frac{j\omega\mu_o}{\tau_z} \sinh \tau_z d \\ \\ \frac{\tau_z}{j\omega\mu_o} \sinh \tau_z d & \cosh \tau_z d \end{bmatrix} \begin{bmatrix} E_z \\ \\ H_\phi \end{bmatrix}_{\rho=\rho_1} \tag{19a}$$

$$\begin{bmatrix} E_\phi \\ \\ H_z \end{bmatrix}_{\rho=\rho_1+d} = \begin{bmatrix} \cosh \tau_\phi d & -\frac{j\omega\mu_o}{\tau_\phi} \sinh \tau_\phi d \\ \\ -\frac{\tau_\phi}{j\omega\mu_o} \sinh \tau_\phi d & \cosh \tau_\phi d \end{bmatrix} \begin{bmatrix} E_\phi \\ \\ H_z \end{bmatrix}_{\rho=\rho_1} \tag{19b}$$

in which $\tau^2_{z,\phi} = j\omega\mu_o\sigma_{z,\phi}$.

We are now in a position to solve our fundamental boundary-value problem. Since this shield is uniform in ϕ and z, we may use the results obtained in the previous section to write, for $a \leq \rho \leq \rho_1$,

$$\hat{\Psi}_o = \frac{\hat{I}}{4} [J_o(\gamma_1\rho)Y_o(\gamma_1 a) - J_o(\gamma_1 a)Y_o(\gamma_1\rho)] \tag{20}$$

and for $\rho \geq \rho_o = \rho_1 + d$, we have

$$\hat{\Psi}_o = \frac{j\omega\varepsilon_o E_o}{\gamma_o^2} \sin\theta \, J_o(\gamma_o\rho) + QH_o^{(2)}(\gamma_o\rho) \tag{21}$$

The first term on the rhs of Eq. (21) is the axially symmetric part of the incident wave, and Q is as yet unknown, as is $\hat{I}$. Constructing the axially symmetric parts $\hat{E}_{zo}$ and $\hat{H}_{\phi o}$ from $\hat{\Psi}_o$ via

$$\hat{E}_{zo} = \frac{\gamma^2}{j\omega\varepsilon} \hat{\Psi}_o \tag{22a}$$

$$\hat{H}_{\phi o} = -\frac{d\hat{\Psi}_o}{d\rho} \tag{22b}$$

and connecting the fields across the shield using Eq. (19a), we find that in the low-frequency limit

$$Q = \frac{\hat{I}_t}{4j} \tag{23a}$$

$$\hat{I} = \left(\cosh \tau_z d + \tau_z \rho_1 \frac{\gamma_1^2}{k_1^2} \ln \frac{\rho_1}{a} \sinh \tau_z d\right)^{-1} \frac{\rho_1}{\rho_o} \hat{I}_t \tag{23b}$$

As a consequence, the function $r(\beta_o)$ is given by

$$r(\beta_o) = \frac{\rho_1}{\rho_0} \left(\cosh \tau_z d + \tau_z \rho_1 \frac{\gamma_1^2}{k_1^2} \ln \frac{\rho_1}{a} \sinh \tau_z d\right)^{-1} \tag{24}$$

Now Z and Z_s may be evaluated using Eqs. (13a) and (13b). We obtain

$$Z = \frac{j\omega\mu_o}{2\pi} \ln \frac{\rho_1}{a} \left(1 + \frac{\coth \tau_z d}{\tau_z \rho_1 \ln \frac{\rho_1}{a}}\right) \tag{25a}$$

$$Z_s = - \frac{j\omega\mu_o}{2\pi \ \tau_z \rho_o} \operatorname{csch} \tau_z d \tag{25b}$$

This completes the formal evaluation of the transmission-line parameters for this shield model. The results are identical to those which we would obtain if the shield were isotropic with conductivity σ_z. One will note that σ_ϕ does not appear in the results because the axially symmetric TE_z and TM_z parts of the electromagnetic field are not coupled by the shield boundary conditions.

If the shield is "good," i.e., if $|\tau_z d| >> 1$, we may write for Z and Z_s the approximate expressions

$$Z \simeq \frac{j\omega\mu_o}{2\pi} \ln \frac{\rho_1}{a} + \frac{j\omega\mu_o}{2\pi \tau_z \rho_1} \tag{26a}$$

$$Z_s \simeq - \frac{j\omega\mu_o}{\pi \tau_z \rho_o} e^{-\tau_z d} \tag{26b}$$

One will note that the shield's anisotropy can change the effectiveness of the shield only for the worse, since if $\sigma_1/\sigma_{11} \leq 1$,

$$|\tau_z d| = |\tau_{zm} d| \left(\cos^2\psi + \frac{\sigma_1}{\sigma_{11}} \sin^2\psi\right)^{1/2} \leq |\tau_{zm} d| \tag{27}$$

where $\tau_{zm}^2 = 2j\omega\mu_o\sigma_{11}$. Curves of $|\tau_z/\tau_{zm}|$ vs. ψ are shown in Figure 2 for various values of the parameter σ_1/σ_{11}. It is evident from these curves that for maximum shielding effectiveness, ψ should be as small as possible and that the contact between the shield wires should be as good as possible, consistent with economy and ease of manufacture. The first observation has also been made by Vance (ref. 2).

It should also be remarked that the presence of an outer dielectric layer on the cable can be easily shown to have no effect on Z and Z_s unless it is electrically thick. A typical weatherproofing layer of carbon-loaded polyethylene is electrically thin at the frequencies of interest, and so does not affect the shielding.

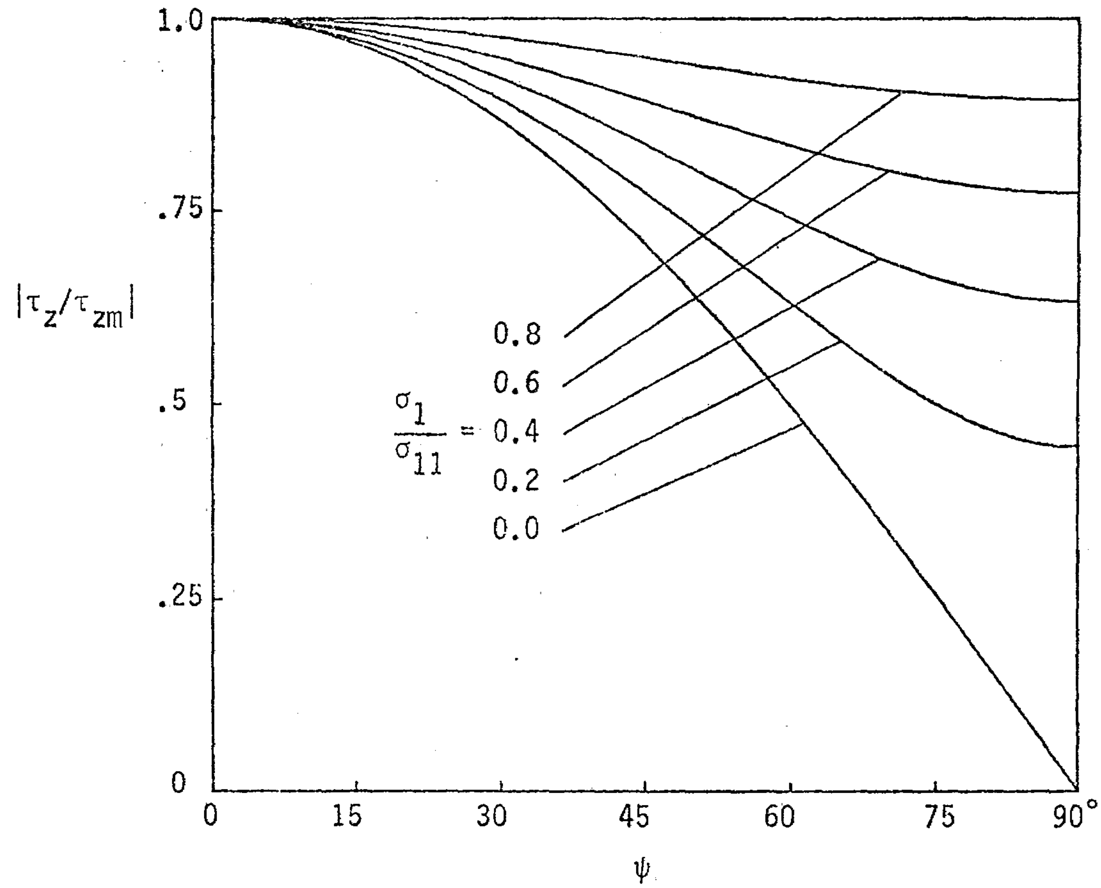

Fig. 2. $|\tau_z/\tau_{zm}|$ vs. ψ for various values of σ_1/σ_{11}.

SECTION IV

SHIELD MODEL B: TWO CONCENTRIC UNIDIRECTIONALLY CONDUCTING SHELLS

In this section we consider a shield model comprising two concentric lossy unidirectionally conducting shells, which are assumed to be physically thin with respect to their radii of curvature, but which are not necessarily electrically thin. Thus the analysis of this model which has been done previously for the lossless case (ref. 3) is extended to the case where a finite resistance in the conduction direction of each shell is allowed. However, we shall limit our consideration to the special case where the shells have the same conductivity in their conduction directions, have no separation between them, and have equal and opposite conduction angles.

Consider first a single unidirectionally conducting shell of inner radius ρ_1 and of thickness $d/2$, where $d << \rho_1$. Let the conduction direction of this shell make an angle ψ with the positive z-direction. (Refer to the (1) - superscripted directions of Fig. 1). The tangential parallel and perpendicular components of a vector field $\bar{A}$ are related to its ϕ and z components by

$$\begin{bmatrix} A_{11} \\ A_1 \end{bmatrix} = \bar{\bar{T}}(\psi) \begin{bmatrix} A_z \\ A_\phi \end{bmatrix} \tag{28}$$

where

$$\bar{\bar{T}}(\psi) = \begin{bmatrix} \cos\psi & \sin\psi \\ -\sin\psi & \cos\psi \end{bmatrix} \tag{29}$$

and $\bar{\bar{T}}^{-1}(\psi) = \bar{\bar{T}}(-\psi)$. Across the shell, the tangential components of $\bar{E}$ and $\bar{H}$ are connected by

$$\begin{bmatrix} E_{11} \\ \\ H_1 \end{bmatrix}_{\rho=\rho_1+d/2} = \begin{bmatrix} \cosh \frac{\tau_c d}{2} & \frac{j\omega\mu_o}{\tau_c} \sinh \frac{\tau_c d}{2} \\ \\ \frac{\tau_c}{j\omega\mu_o} \sinh \frac{\tau_c d}{2} & \cosh \frac{\tau_c d}{2} \end{bmatrix} \begin{bmatrix} E_{11} \\ \\ H_1 \end{bmatrix}_{\rho=\rho_1} \tag{30a}$$

$$\begin{bmatrix} E_1 \\ \\ H_{11} \end{bmatrix}_{\rho=\rho_1+d/2} = \begin{bmatrix} E_1 \\ \\ H_{11} \end{bmatrix}_{\rho=\rho_1} \tag{30b}$$

where $\tau_c^2 = j\omega\mu_o\sigma_c$, with σ_c denoting the conductivity of the shell material in the conduction direction.

We may now construct the boundary conditions across the shield layer in terms of the ϕ and z components of the electric and magnetic fields. By transforming the ϕ and z component representations of $\bar{E}$ and $\bar{H}$ into representations in terms of parallel and perpendicular components, applying Eq. (30) to these, and then transforming back to a cylindrical coordinate representation, we obtain for a single shield layer the relation

$$\begin{bmatrix} E_z \\ E_\phi \\ H_z \\ H_\phi \end{bmatrix}_{\rho=\rho_1+d/2} = \begin{bmatrix} \bar{\bar{T}}(-\psi) & \bar{\bar{0}} \\ \bar{\bar{0}} & \bar{\bar{T}}(-\psi) \end{bmatrix} \begin{bmatrix} \bar{\bar{B}}_{11} & \bar{\bar{B}}_{12} \\ \bar{\bar{B}}_{21} & \bar{\bar{B}}_{22} \end{bmatrix} \begin{bmatrix} \bar{\bar{T}}(\psi) & \bar{\bar{0}} \\ \bar{\bar{0}} & \bar{\bar{T}}(\psi) \end{bmatrix} \begin{bmatrix} E_z \\ E_\phi \\ H_z \\ H_\phi \end{bmatrix}_{\rho=\rho_1} \tag{31}$$

$\bar{\bar{0}}$ denotes a 2×2 null matrix and

$$\bar{\bar{B}}_{11} = \begin{bmatrix} \cosh \frac{\tau_c d}{2} & 0 \\ \\ 0 & 1 \end{bmatrix} \tag{32a}$$

$$\overline{\overline{B}}_{12} = \begin{bmatrix} 0 & \dfrac{j\omega\mu_o}{\tau_c} \sinh \dfrac{\tau_c d}{2} \\ 0 & 0 \end{bmatrix} \tag{32b}$$

$$\overline{\overline{B}}_{21} = \begin{bmatrix} 0 & 0 \\ \dfrac{\tau_c}{j\omega\mu_o} \sinh \dfrac{\tau_c d}{2} & 0 \end{bmatrix} \tag{32c}$$

$$\overline{\overline{B}}_{22} = \begin{bmatrix} 1 & 0 \\ 0 & \cosh \dfrac{\tau_c d}{2} \end{bmatrix} \tag{32d}$$

Let us introduce the shorthand notation

$$\overline{\overline{K}}(\psi) = \begin{bmatrix} \overline{\overline{T}}(-\psi) & \overline{\overline{0}} \\ \overline{\overline{0}} & \overline{\overline{T}}(-\psi) \end{bmatrix} \begin{bmatrix} \overline{\overline{B}}_{11} & \overline{\overline{B}}_{12} \\ \overline{\overline{B}}_{21} & \overline{\overline{B}}_{22} \end{bmatrix} \begin{bmatrix} \overline{\overline{T}}(\psi) & \overline{\overline{0}} \\ \overline{\overline{0}} & \overline{\overline{T}}(\psi) \end{bmatrix} \tag{33}$$

and

$$\overline{E} = \begin{bmatrix} E_z \\ E_\phi \end{bmatrix} \tag{34a}$$

$$\overline{H} = \begin{bmatrix} H_z \\ H_\phi \end{bmatrix} \tag{34b}$$

Then for a single shell,

$$\begin{bmatrix} \overline{E} \\ \overline{H} \end{bmatrix}_{\rho=\rho_1+d/2} = \overline{\overline{K}}(\psi) \begin{bmatrix} \overline{E} \\ \overline{H} \end{bmatrix}_{\rho=\rho_1} \tag{35}$$

Now if the shield comprises two concentric unidirectionally conducting shells of equal thickness and with equal and opposite conduction angles, the connection between the fields inside and outside the shield is given by

$$\begin{bmatrix} \bar{E} \\ \bar{H} \end{bmatrix}_{\rho=\rho_1+d} = \bar{\bar{K}}(-\psi)\ \bar{\bar{K}}(\psi) \begin{bmatrix} \bar{E} \\ \bar{H} \end{bmatrix}_{\rho=\rho_1} \tag{36}$$

Thus, if

$$\bar{\bar{\Gamma}}(\psi) \equiv \bar{\bar{K}}(-\psi)\ \bar{\bar{K}}(\psi) \tag{37}$$

we have

$$\begin{bmatrix} \bar{E} \\ \bar{H} \end{bmatrix}_{\rho=\rho_1+d} = \bar{\bar{\Gamma}}(\psi) \begin{bmatrix} \bar{E} \\ \bar{H} \end{bmatrix}_{\rho=\rho_1} \tag{38}$$

in which

$$\Gamma_{11} = \cosh \tau_c d \cos 2\psi \cos^2\psi + \cosh \frac{\tau_c d}{2} \sin^2 2\psi - \cos 2\psi \sin^2\psi \tag{39a}$$

$$\Gamma_{12} = \frac{1}{4}\left(\cosh \tau_c d - 2\cosh \frac{\tau_c d}{2} + 1\right)\sin 4\psi \tag{39b}$$

$$\Gamma_{13} = -\frac{1}{2}\frac{j\omega\mu_o}{\tau_c} \sinh \frac{\tau_c d}{2}\left(\cosh \frac{\tau_c d}{2} - 1\right)\sin 4\psi \tag{39c}$$

$$\Gamma_{14} = \frac{j\omega\mu_o}{\tau_c} \sinh \frac{\tau_c d}{2}\left(\sin^2 2\psi + 2\cosh \frac{\tau_c d}{2} \cos 2\psi \cos^2\psi\right) \tag{39d}$$

$$\Gamma_{21} = -\frac{1}{4}\left(\cosh \tau_c d - 2\cosh \frac{\tau_c d}{2} + 1\right)\sin 4\psi \tag{39e}$$

$$\Gamma_{22} = -\cosh \tau_c d \cos 2\psi \sin^2\psi + \cosh \frac{\tau_c d}{2} \sin^2 2\psi + \cos 2\psi \cos^2\psi \tag{39f}$$

$$\Gamma_{23} = -\frac{j\omega\mu_o}{\tau_c} \sinh\frac{\tau_c d}{2}\left(\sin^2 2\psi - 2\cosh\frac{\tau_c d}{2}\cos 2\psi\,\sin^2\psi\right) \tag{39g}$$

$$\Gamma_{24} = -\frac{1}{2}\frac{j\omega\mu_o}{\tau_c} \sinh\frac{\tau_c d}{2}\left(\cosh\frac{\tau_c d}{2} - 1\right)\sin 4\psi \tag{39h}$$

$$\Gamma_{31} = \frac{1}{2}\frac{\tau_c}{j\omega\mu_o} \sinh\frac{\tau_c d}{2}\left(\cosh\frac{\tau_c d}{2} - 1\right)\sin 4\psi \tag{39i}$$

$$\Gamma_{32} = -\frac{\tau_c}{j\omega\mu_o} \sinh\frac{\tau_c d}{2}\left(\sin^2 2\psi - 2\cosh\frac{\tau_c d}{2}\cos 2\psi\,\sin^2\psi\right) \tag{39j}$$

$$\Gamma_{33} = -\cosh\tau_c d\,\cos 2\psi\,\sin^2\psi + \cosh\frac{\tau_c d}{2}\sin^2 2\psi + \cos 2\psi\,\cos^2\psi \tag{39k}$$

$$\Gamma_{34} = \frac{1}{4}\left(\cosh\tau_c d - 2\cosh\frac{\tau_c d}{2} + 1\right)\sin 4\psi \tag{39ℓ}$$

$$\Gamma_{41} = \frac{\tau_c}{j\omega\mu_o} \sinh\frac{\tau_c d}{2}\left(\sin^2 2\psi + 2\cosh\frac{\tau_c d}{2}\cos 2\psi\,\cos^2\psi\right) \tag{39m}$$

$$\Gamma_{42} = \frac{1}{2}\frac{\tau_c}{j\omega\mu_o}\left(\cosh\frac{\tau_c d}{2} - 1\right)\sin 4\psi\,\sinh\frac{\tau_c d}{2} \tag{39n}$$

$$\Gamma_{43} = -\frac{1}{4}\left(\cosh\tau_c d - 2\cosh\frac{\tau_c d}{2} + 1\right)\sin 4\psi \tag{39o}$$

$$\Gamma_{44} = \cosh\tau_c d\,\cos 2\psi\,\cos^2\psi + \cosh\frac{\tau_c d}{2}\sin^2 2\psi - \cos 2\psi\,\sin^2\psi \tag{39p}$$

We are now in a position to solve the boundary-value problem of plane-wave scattering by the structure. Since the TE_z and TM_z parts of the axially symmetric portion of the electromagnetic field are evidently coupled by the boundary conditions at the shield, we shall consider both parts of the field to be present and write, for $a \le \rho \le \rho_1$,

$$\hat{\Psi}_o^{(i)} = \frac{\hat{I}}{4}\left[J_o(\gamma_1\rho)Y_o(\gamma_1 a) - J_o(\gamma_1 a)Y_o(\gamma_1\rho)\right] \tag{40a}$$

$$\hat{\Phi}_o^{(i)} = \frac{P}{4}\left[J_o(\gamma_1\rho)Y_o'(\gamma_1 a) - J_o'(\gamma_1 a)Y_o(\gamma_1\rho)\right] \tag{40b}$$

and for $\rho \geq \rho_o = \rho_1 + d$,

$$\hat{\Psi}_o^{(o)} = \frac{j\omega\varepsilon_o E_o \sin\theta}{\gamma_o^2} J_o(\gamma_o\rho) + QH_o^{(2)}(\gamma_o\rho) \tag{41a}$$

$$\hat{\Phi}_o^{(o)} = SH_o^{(2)}(\gamma_o\rho) \tag{41b}$$

in which $\hat{I}$, P, Q, and S are unknown. It is now necessary merely to construct the axially symmetric parts of $\bar{E}$ and $\bar{H}$ on each side of the shield and then to connect them across the shield using Eqs. (38) and (39). The resulting four equations may then be solved for any of the unknowns $\hat{I}$, P, S, or Q.

The tangential field components are obtained from $\hat{\Psi}_o$ and $\hat{\Phi}_o$ via the relations

$$\hat{E}_{\phi o} = \frac{d\hat{\Phi}_o}{d\rho} \tag{42a}$$

$$\hat{E}_{zo} = \frac{\gamma^2}{j\omega\varepsilon}\hat{\Psi}_o \tag{42b}$$

$$\hat{H}_{\phi o} = -\frac{d\hat{\Psi}_o}{d\rho} \tag{42c}$$

$$\hat{H}_{zo} = \frac{\gamma^2}{j\omega\mu}\hat{\Phi}_o \tag{42d}$$

and after the tedious but straightforward process of solving for the unknown of interest $\hat{I}$ in the low-frequency limit, we obtain

$$r(\beta_o) = \frac{A}{\frac{\gamma_1^2}{k_1^2} B + C} \tag{43}$$

in which

$$A = \frac{2}{\pi\rho_o} \left(\tau_c W_1 \Gamma'_{32} - \frac{2}{\pi a} \Gamma_{33}\right) \tag{44a}$$

$$B = \frac{2\tau_c W_2}{\pi a} \left(\Gamma'_{31}\Gamma_{43} - \Gamma'_{41}\Gamma_{33}\right) - \tau_c^2 W_1 W_2 \left(\Gamma'_{31}\Gamma'_{42} - \Gamma'_{41}\Gamma'_{32}\right) \tag{44b}$$

$$C = \left(\frac{2}{\pi}\right)^2 \frac{1}{a\rho_1} \left(\Gamma_{43}\Gamma_{34} - \Gamma_{33}\Gamma_{44}\right) + \frac{2\tau_c W_1}{\pi\rho_1} \left(\Gamma_{44}\Gamma'_{32} - \Gamma_{34}\Gamma'_{42}\right) \tag{44c}$$

where

$$\Gamma_{31,32,41,42} = \frac{\tau_c}{j\omega\mu_o} \Gamma'_{31,32,41,42} \tag{45a}$$

$$W_1 = \frac{1}{\pi} \left(\frac{\rho_1}{a} - \frac{a}{\rho_1}\right) \tag{45b}$$

$$W_2 = \frac{2}{\pi} \ln \frac{\rho_1}{a} \tag{45c}$$

Z and Z_s are now obtained from Eqs. (13a) and (13b):

$$Z = \frac{j\omega\mu_o}{2\pi} \ln \frac{\rho_1}{a} \left(1 + \frac{C}{B}\right) \tag{46a}$$

$$Z_s = - \frac{j\omega\mu_o}{2\pi} \ln \frac{\rho_1}{a} \frac{A}{B} \tag{46b}$$

Under the conditions $\tau_c d >> 1$, $\psi \neq 0$ or $\pi/4$, we obtain the following approximate results:

$$A \simeq \frac{\tau_c e^{\tau_c d}}{\pi^2 a} \cos 2\psi \sin^2\psi \left(1 - \frac{a^2}{\rho_1^2}\right) \left(\frac{\rho_1}{\rho_o}\right) \tag{47a}$$

$$B \simeq - \frac{\tau_c^2}{2\pi^2} \frac{\rho_1}{a} \ln \frac{\rho_1}{a} \left(1 - \frac{a^2}{\rho_1^2}\right) e^{\tau_c d} \sin^2 2\psi \tag{47b}$$

$$C \simeq \frac{\tau_c}{2\pi^2 a} \left(1 - \frac{a^2}{\rho_1^2}\right) (\cos^3 2\psi - 1) e^{\tau_c d} \tag{47c}$$

so that

$$Z \simeq \frac{j\omega\mu_o}{2\pi} \ln\frac{\rho_1}{a}\left[1 + \frac{1}{\tau_c\rho_1 \ln\frac{\rho_1}{a}} f(\psi)\right] \tag{48a}$$

$$Z_s \simeq \frac{j\omega\mu_o}{2\pi}\frac{1}{\tau_c\rho_o} g(\psi) \tag{48b}$$

where

$$f(\psi) = \frac{1-\cos^3\psi}{\sin^2 2\psi} = \cos 2\psi + \frac{1}{1+\cos 2\psi} \tag{49a}$$

$$g(\psi) = \frac{\cos 2\psi}{1+\cos 2\psi} \tag{49b}$$

The functions $f(\psi)$ and $g(\psi)$ are shown in Figures 3 and 4. In the event that $\psi = 0$ or $\pi/4$, we have the following results:

$$\psi = 0: \quad Z = \frac{j\omega\mu_o}{2\pi}\ln\frac{\rho_1}{a}\left(1 + \frac{\coth \tau_c d}{\tau_c\rho_1 \ln\frac{\rho_1}{a}}\right) \tag{50a}$$

$$Z_s = -\frac{j\omega\mu_o}{2\pi}\frac{1}{\tau_c\rho_o} \operatorname{csch} \tau_c d \tag{50b}$$

$$\psi = \frac{\pi}{4}: \quad Z = \frac{j\omega\mu_o}{2\pi}\ln\frac{\rho_1}{a}\left(1 + \frac{\coth \frac{\tau_c d}{2}}{\tau_c\rho_1 \ln\frac{\rho_1}{a}}\right) \tag{51a}$$

$$Z_s = -\frac{j\omega\mu_o}{2\pi\tau_c\rho_o} \operatorname{csch} \frac{\tau_c d}{2} \tag{51b}$$

Thus one will note that the transfer impedance Z_s decreases exponentially with $\tau_c d$ only when $\psi = 0$ or $\pi/4$; otherwise it decreases only algebraically. A comparison of these results with those of the previous section would indicate the importance of actually braiding a shield, rather than constructing it of two separate layers.

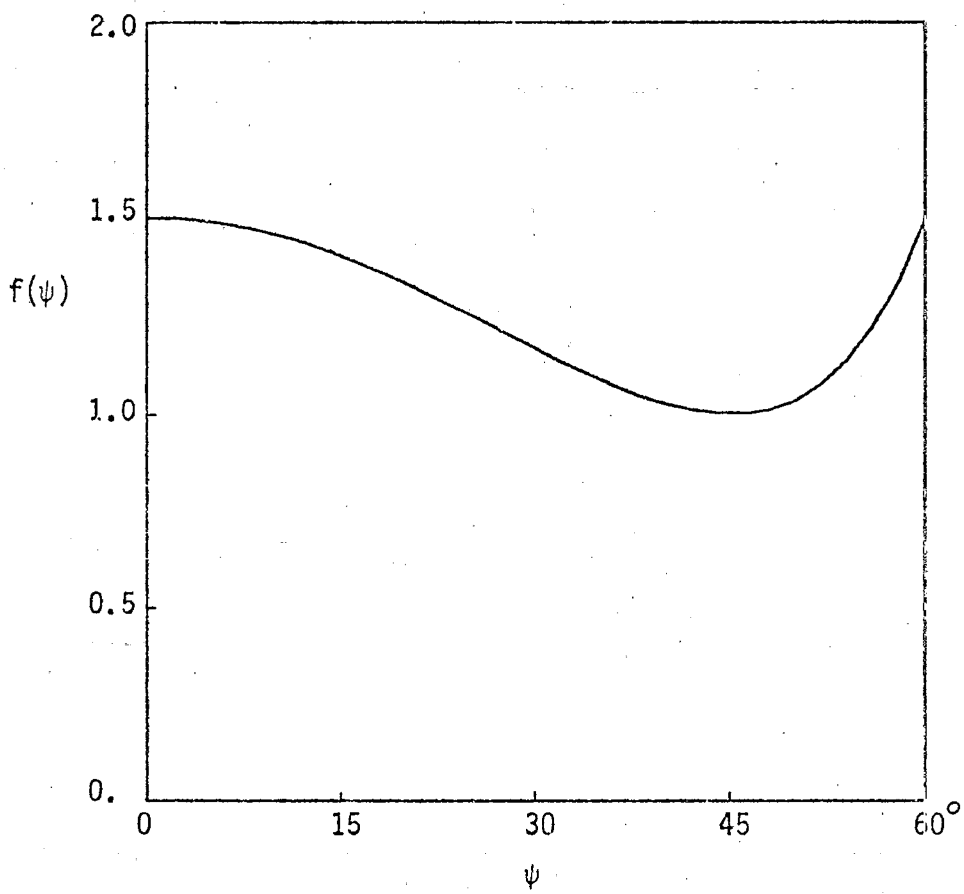

Fig. 3. $f(\psi)$ vs. ψ.

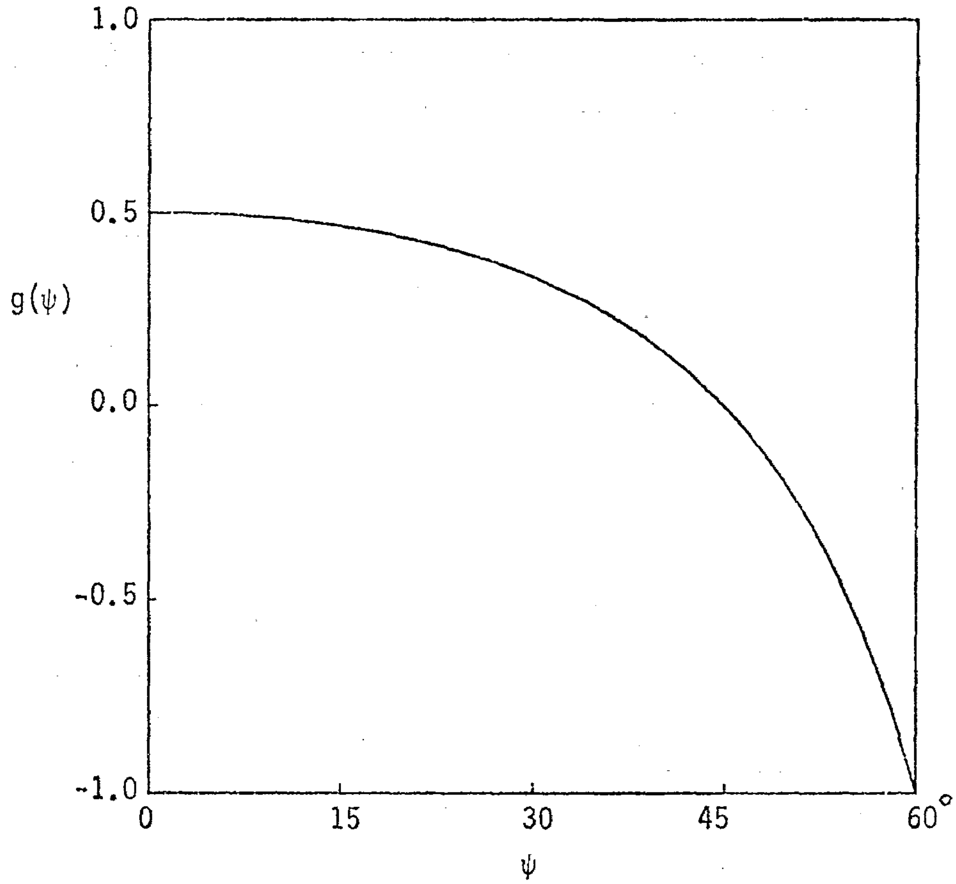

Fig. 4. $g(\psi)$ vs. ψ.

As in the previous shield model considered, the presence of an exterior dielectric jacket can be shown to have no effect on Z or Z_s, as long as it is electrically thin.

SECTION V

SHIELD MODEL C: TWO COUNTERWOUND M-FILAR FILAMENTARY HELICES SURROUNDED BY A DIELECTRIC JACKET

We consider in this section a coaxial-cable model comprising as before a perfectly conducting cylinder of radius a as center conductor surrounded by a lossless dielectric of permittivity ε_1 for $a \leq \rho \leq \rho_1$. At $\rho = \rho_1$ is located a pair of M-filar counterwound filamentary helices, each filament of which is an imperfectly conducting wire of radius b, where $b \ll \rho_1$. The filaments themselves make an angle ψ with respect to the positive z-axis. A (possibly lossy) dielectric jacket of permittivity ε_2 surrounds the helices and extends to $\rho = \rho_o \geq \rho_1$. The geometry of the model is shown in Fig. (5). As in the cases considered previously, the cable is illuminated with a low-frequency TM_z-polarized plane wave incident at an angle θ with respect to the z-axis. The cable parameters are to be obtained from the solution of the scattering problem.

Of particular interest in this problem is the effect of the dielectric jacket around the cable on the cable parameters and on the shielding effectiveness. In the other two cases considered in this report, the azimuthal and axial uniformity of the shield determined the values of Y and Γ_s to be those given in Eqs. (14a) and (14b). Since this assumption is not applicable for the present shield model, we expect Y and Γ_s to take on values different from those obtained previously, and to depend upon ε_2 as well as upon ε_1, since the electric field can penetrate the apertures in the shield. We particularly expect that $\Gamma_s \neq 0$ unless the conductivity of the dielectric jacket is sufficient to obscure the effects of the individual shield filaments. Additionally, one would not expect that Z and Z_s will

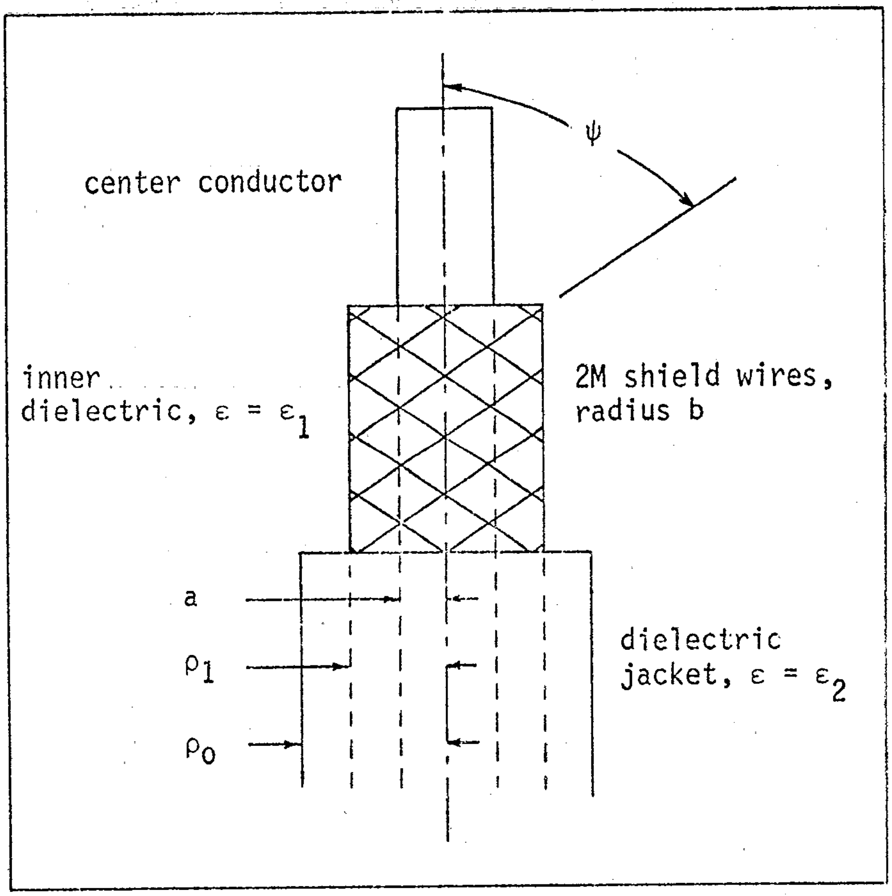

Fig. 5. Geometry of multifilar helix shielded cable.

depend upon ε_2 as long as the jacket does not carry any appreciable current, compared to the currents in the shield wires.

The approach to be taken in solving this problem is one involving two steps. In the first step, the shield conductors are assumed to be absent and we shall obtain the "primary" current on the center conductor and the potential difference developed across the inner dielectric, when the cable is illuminated by an incident plane wave. In the second step, the fields created by the filamentary currents on the shield conductors will be obtained in terms of these (unknown) currents. Then by imposing an impedance condition at the wire surfaces the two problems are connected; and the cable parameters may then be obtained.

The first problem is very simple. We obtain the following results:

<u>primary center-conductor current:</u> $$\hat{I}_p = \frac{4E_o}{\eta_o\gamma_o\, H_o^{(2)}(\gamma_o\rho_o)} \tag{52a}$$

<u>total primary current:</u> $$\hat{I}_{tp} = \hat{I}_p \tag{52b}$$

<u>primary potential difference:</u> $$\hat{V}_p = \frac{\beta_o}{2\pi\omega\varepsilon_1}\,\ell n\,\frac{\rho_1 - b}{a}\,\hat{I}_p \tag{52c}$$

<u>total primary charge per unit length:</u> $$\hat{Q}_p = \frac{\beta_o}{\omega}\,\hat{I}_p \tag{52d}$$

<u>primary tangential electric field at $\rho = \rho_1 - b$:</u> $$\hat{E}_{zp} = \frac{-\gamma_1^2}{2\pi j\omega\varepsilon_1}\,\ell n\,\frac{\rho_1 - b}{a}\,\hat{I}_p \tag{52e}$$

$$\hat{E}_{\phi p} = 0 \tag{52f}$$

The second problem is a little more involved. The fundamental assumption to be made is that each filament carries the same current I_o, where

$$I_o = \hat{I}_o e^{-j\beta_o z} \tag{53}$$

The assumption that all filamentary currents are identical is valid in the low-frequency limit since the dominant term in the incident-wave expansion at low frequencies is axially symmetric, so that each wire is excited identically; and the neglect of the space harmonics of the filamentary currents is justified also by the fact that we intend to consider only the low-frequency case where the period of the shield structure is much less than the axial wavelength.

Consider first the case where M = 1, i.e., there is only one pair of conductors in the shield, located at $\rho = \rho_1$, $\phi = \pm z/\rho_1 \tan\psi$. We obtain the electric and magnetic fields $\bar{E}$ and $\bar{H}$ from the functions Ψ and Φ as indicated in Eq. (8); since the shield is periodic in ϕ with period 2π and in z with period $p = 2\pi\rho_1 \cot\psi$, appropriate Floquet forms for Ψ and Φ are the following:

$$\begin{bmatrix} \Psi \\ \Phi \end{bmatrix} = \sum_{n=-\infty}^{\infty} \sum_{m=-\infty}^{\infty} \begin{bmatrix} \hat{\Psi}_{nm} \\ \hat{\Phi}_{nm} \end{bmatrix} e^{jn\phi - j\beta_m z} \tag{54}$$

$\hat{\Psi}_{nm}$ and $\hat{\Phi}_{nm}$ are functions only of ρ, and

$$\beta_m = \beta_o + \frac{2m\pi}{p} \tag{55}$$

Appropriate forms for $\hat{\Psi}_{nm}$ and $\hat{\Phi}_{nm}$ in each region are as follows:

<u>$a \le \rho < \rho_1$:</u>

$$\hat{\Psi}_{nm1} = A_{nm}[I_n(\lambda_{m1}\rho)K_n(\lambda_{m1}a) - I_n(\lambda_{m1}a)K_n(\lambda_{m1}\rho)] \tag{56a}$$

$$\hat{\Phi}_{nm1} = B_{nm}[I_n(\lambda_{m1}\rho)K_n'(\lambda_{m1}a) - I_n'(\lambda_{m1}a)K_n(\lambda_{m1}\rho)] \tag{56b}$$

$\underline{\rho_1 < \rho \leq \rho_o}$:

$$\hat{\Psi}_{nm2} = C_{nm} I_n(\lambda_{m2}\rho) + D_{nm} K_n(\lambda_{m2}\rho) \tag{57a}$$

$$\hat{\Phi}_{nm2} = E_{nm} I_n(\lambda_{m2}\rho) + F_{nm} K_n(\lambda_{m2}\rho) \tag{57b}$$

$\underline{\rho \geq \rho_o}$:

$$\hat{\Psi}_{nmo} = G_{nm} K_n(\lambda_{mo}\rho) \tag{58a}$$

$$\hat{\Phi}_{nmo} = H_{nm} K_n(\lambda_{mo}\rho) \tag{58b}$$

where

$$\lambda_{m1}^2 = \beta_m^2 - k_1^2 \tag{59a}$$

$$\lambda_{m2}^2 = \beta_m^2 - k_2^2 \tag{59b}$$

$$\lambda_{mo}^2 = \beta_m^2 - k_o^2 \tag{59c}$$

Now in order to solve for the unknown coefficients $A_{nm} - H_{nm}$ in terms of the unknown currents $\hat{I}_o$ one merely needs to ensure continuity of tangential $\bar{E}$ and $\bar{H}$ at $\rho = \rho_o$, and tangential $\bar{E}$ at $\rho = \rho_1$; and to ensure the appropriate discontinuity of tangential $\bar{H}$ at $\rho = \rho_1$. The surface current density represented by the shield filaments is easily shown to be

$$\bar{J}_s = \sum_{n=-\infty}^{\infty} \sum_{m=-\infty}^{\infty} (\hat{J}_{sznm} \bar{a}_z + \hat{J}_{s\phi nm} \bar{a}_\phi) e^{jn\phi - j\beta_m z} \tag{60}$$

in which

$$\hat{J}_{sznm} = \frac{\hat{I}_o \cos\psi}{2\pi\rho_1} [\delta_k(n-m) + \delta_k(n+m)] \tag{61a}$$

$$\hat{J}_{s\phi nm} = \frac{\hat{I}_o \sin\psi}{2\pi\rho_1} [\delta_k(n-m) - \delta_k(n+m)] \tag{61b}$$

where $\delta_k(\cdot)$ denotes the Kronecker delta-function. It is evident from Eqs. (61) that only those coefficients $A_{nm} - H_{nm}$ for which n=m or n=-m will be nonzero. Further, each nonzero coefficient is directly proportional to $\hat{I}_o$.

In the event that more helix pairs are added to the shield, symmetrically spaced around the z-axis, the coefficients $\hat{J}_{sznm}$ and $\hat{J}_{s\phi nm}$ are multiplied by M, the number of helix pairs, and by $\delta_k(n-kM)$, where k is any integer. We now have all the information necessary to solve for the unknown coefficients $A_{nm} - H_{nm}$ in terms of $\hat{I}_o$ and thus to obtain the solution to the second phase of our problem. Let us now presume that this has been done (details are given in the Appendix) and write, e.g., $A_{nm} = M\hat{I}_o A'_{nm}$ as appropriate, understanding that the allowed values of n are kM, where k is any integer.

The coupling of the primary field to the grid-induced field will now be carried out. Let us denote by $\hat{E}_+$ the component of the total electric field parallel to the right-handed helix wires:

$$\hat{E}_+ = \sin\psi\ \hat{E}_\phi + \cos\psi\ \hat{E}_z \tag{62}$$

Evaluating this component of electric field at $\rho = \rho_1 - b$, $\phi = 2\pi z/p$, and equating it to $Z_w\hat{I}_o$, where Z_w is the wire impedance per unit length, we have

$$\sum_{\substack{n=-\infty \\ n=kM}}^{\infty} \sum_{m=-\infty}^{\infty} e^{j\frac{2\pi z}{p}(n-m)} \left[\left(\frac{n\beta_m \sin\psi}{\rho_1} - \lambda_{m1}^2 \cos\psi\right) \frac{\hat{I}_o M A'_{nm}}{j\omega\varepsilon_1} L_{1nm}^{(-)} + \lambda_{m1} \sin\psi\ \hat{I}_o B'_{nm} M\ L_{4nm}^{(-)}\right] - \frac{1}{2\pi} \frac{\gamma_1^2}{j\omega\varepsilon_1} \cos\psi\ \ln\frac{\rho_1}{a}\ \hat{I}_p = Z_w\hat{I}_o \tag{63}$$

in which b is neglected with respect to ρ_1 everywhere except in $L_{1nm}^{(-)}$ and $L_{4nm}^{(-)}$, where

$$L_{1nm}^{(-)} = I_n[\lambda_{m1}(\rho_1-b)]K_n(\lambda_{m1}a) - I_n(\lambda_{m1}a)K_n[\lambda_{m1}(\rho_1-b)] \tag{64a}$$

$$L_{4nm}^{(-)} = I_n'[\lambda_{m1}(\rho_1-b)]K_n'(\lambda_{m1}a) - I_n'(\lambda_{m1}a)K_n'[\lambda_{m1}(\rho_1-b)] \tag{64b}$$

and Z_w is given by

$$Z_w = \frac{\eta_w}{2\pi b}\frac{I_o(\tau_w b)}{I_1(\tau_w b)} \tag{65}$$

with $\eta_w = (j\omega\mu_o/\sigma_w)^{1/2}$, where σ_w denotes the wire conductivity and $\tau_w^2 = j\omega\mu_o\sigma_w$. Considering only the n=m terms in the double summation in Eq. (63), we have after a little algebra the total shield current $\hat{I}_s$:

$$\frac{\hat{I}_s}{\hat{I}_p} = \left\{1 + \frac{Z_w}{j\omega\mu_o M}\left(\frac{\gamma_1^2}{\pi k_1^2}\cos^2\psi \,\ln\frac{\rho_1}{a}\right)^{-1}\right.$$

$$+ \left(\frac{\gamma_1^2}{\pi k_1^2}\cos^2\psi \,\ln\frac{\rho_1}{a}\right)^{-1} \sum_{\substack{k=-\infty \\ k\neq 0 \\ n=kM}}^{\infty} \left[\left(\frac{n\beta_n \sin\psi}{\rho_1} - \lambda_{n1}^2 \cos\psi\right)\frac{A_{nn}'L_{1nn}^{(-)}}{k_1^2}\right.$$

$$\left.\left. - \lambda_{n1}\frac{B_{nn}'L_{4nn}^{(-)}}{j\omega\mu_o}\sin\psi\right]\right\}^{-1} \tag{66}$$

We have made use of the facts that $A_{oo}' = \frac{1}{\pi}\cos\psi$, $B_{oo}' = 0$ (see the Appendix); $\lambda_{01}^2 = -\gamma_1^2$ (by definition); $L_{100}^{(-)} = \ln(\rho_1-b)/a$ in the low-frequency limit; and $\hat{I}_s = 2M\hat{I}_o\cos\psi$.

Now the total current on the center conductor, $\hat{I}_c$, is just the sum of $\hat{I}_p$ and the current induced on the center conductor by the grid, and is easily shown to be

$$\hat{I}_c = \hat{I}_p - 2\pi M\hat{I}_o A_{oo}' = \hat{I}_p - \hat{I}_s \tag{67}$$

Furthermore, the total current on the structure is given by

$$\hat{I}_t = \hat{I}_p + \hat{I}_s - 2\pi M \hat{I}_o A'_{oo} = \hat{I}_p \tag{68}$$

The ratio of total center-conductor current to total current is then given by

$$r(\beta_o) = \frac{\hat{I}_c}{\hat{I}_p} = \frac{F(\beta_o) + \dfrac{Z_w}{j\omega\mu_o M}}{F(\beta_o) + \dfrac{Z_w}{j\omega\mu_o M} + \dfrac{\gamma_1^2}{\pi k_1^2} \cos^2\psi \, \ln \dfrac{\rho_1}{a}} \tag{69}$$

where

$$F(\beta_o) \equiv \sum_{\substack{k=-\infty \\ k\neq 0 \\ n=kM}}^{\infty} \left[\left(\frac{n\beta_n \sin\psi}{\rho_1} - \lambda_{n1}^2 \cos\psi \right) \frac{A'_{nn} L^{(-)}_{1nn}}{k_1^2} - \lambda_{n1} \sin\psi \frac{B'_{nn} L^{(-)}_{4nn}}{j\omega\mu_o} \right] \tag{70}$$

That portion of the potential of the center conductor with respect to the shield radius ρ_1-b which is due to the shield currents is given by

$$\hat{V}_g = - \frac{M\hat{I}_o}{\omega\varepsilon_1} \sum_{\substack{n=-\infty \\ n=kM}}^{\infty} \sum_{m=-\infty}^{\infty} \beta_m A_{nm} L^{(-)}_{1nm} \, e^{jn\phi - j2\pi mz/p} \tag{71}$$

On an individual right-hand helix wire, $\phi = 2\pi z/p$; thus

$$\hat{V}_g = - \frac{\beta_o}{2\pi\omega\varepsilon_1} \ln \frac{\rho_1}{a} \hat{I}_s - \frac{\beta_o \pi \sec\psi}{2\pi\omega\varepsilon_1} \hat{I}_s \, G(\beta_o) \tag{72}$$

where

$$G(\beta_o) \equiv \sum_{\substack{k=-\infty \\ k\neq 0 \\ n=kM}}^{\infty} \frac{\beta_n}{\beta_o} A'_{nn} L^{(-)}_{1nn} \tag{73}$$

The total potential on the center conductor with respect to the shield is therefore

$$\hat{V}_c = \hat{V}_g + \hat{V}_p = \frac{\beta_o}{2\pi\omega\varepsilon_1} \left\{ \left[\ln \frac{\rho_1}{a} + \pi \sec\psi \, G(\beta_o) \right] \hat{I}_c - \pi \sec\psi \, G(\beta_o) \hat{I}_p \right\} \tag{74}$$

so that

$$s(\beta_o) = \frac{1}{2\pi\omega\varepsilon_1}\left\{\left[\ell n\,\frac{\rho_1}{a} + \pi\sec\psi\; G(\beta_o)\right] r(\beta_o) - \pi\sec\psi\; G(\beta_o)\right\} \tag{75}$$

Having obtained $r(\beta_o)$ and $s(\beta_o)$, we may now obtain the transmission-line parameters Z, Z_s, Y, and Γ_s. We have

$$r(0) = \frac{F(0) + \dfrac{Z_w}{j\omega\mu_o M}}{F(0) + \dfrac{Z_w}{j\omega\mu_o M} + \dfrac{1}{\pi}\cos^2\psi\;\ell n\,\dfrac{\rho_1}{a}} \tag{76a}$$

$$r(k_1) = 1 \tag{76b}$$

$$s(0) = \frac{1}{2\pi\omega\varepsilon_1}\left\{r(0)\,\ell n\,\frac{\rho_1}{a} + \pi\sec\psi\; G(0)\,[r(0) - 1]\right\} \tag{76c}$$

$$s(k_1) = \frac{1}{2\pi\omega\varepsilon_1}\;\ell n\,\frac{\rho_1}{a} \tag{76d}$$

and therefore, from Eqs. (7), we obtain

$$Z = \frac{j\omega\mu_o}{2\pi}\;\ell n\,\frac{\rho_1}{a}\left[1 + \frac{\pi\sec^2\psi}{\ell n\,\dfrac{\rho_1}{a}}\left(F(0) + \frac{Z_w}{j\omega\mu_o M}\right)\right] \tag{77a}$$

$$Z_s = -\frac{j\omega\mu_o}{2}\;\sec^2\psi\left(F(0) + \frac{Z_w}{j\omega\mu_o M}\right) \tag{77b}$$

$$Y = \frac{j\omega 2\pi\varepsilon_1}{\ell n\,\dfrac{\rho_1}{a}}\left(1 + \frac{\pi\sec\psi}{\ell n\,\dfrac{\rho_1}{a}}\;G(0)\right)^{-1} \tag{77c}$$

$$\Gamma_s = -\frac{\pi\sec\psi}{\ell n\,\dfrac{\rho_1}{a}}\;G(0)\left[1 + \frac{\pi\sec\psi}{\ell n\,\dfrac{\rho_1}{a}}\;G(0)\right]^{-1} \tag{77d}$$

The evaluation of $F(0)$ and $G(0)$ in the low-frequency limit is carried out in the Appendix, with the following results: if $1-a/\rho_1$ and $\rho_o/\rho_1 - 1$ are not too small and if $M >> 1$, then

$$F(0) = -\frac{\cos\psi}{2\pi M} \ln\left(1 - e^{-\pi c/2}\right) \tag{78a}$$

$$G(0) = -\frac{\varepsilon_1 \cos^2\psi}{\pi M(\varepsilon_1 + \varepsilon_2)} \ln\left(1 - e^{-\pi c/2}\right) \tag{78b}$$

c denotes the optical coverage of the shield

$$c = \frac{2Mb}{\pi\rho_1} \sec\psi \leq 1 \tag{79}$$

In order that the assumption of continuity of the tangential electric field through the wire grid be valid, $c \ll 1$, in which case

$$F(0) \simeq \frac{\cos\psi}{2\pi M} \ln\left(\frac{2}{\pi c}\right) \tag{80a}$$

$$G(0) \simeq \frac{\varepsilon_1 \cos^2\psi}{\pi M(\varepsilon_1 + \varepsilon_2)} \ln\left(\frac{2}{\pi c}\right) \tag{80b}$$

Thus explicit forms for Z, Z_s, Y, and Γ_s are given in the low-frequency limit by

$$Z = \frac{j\omega\mu_o}{2\pi} \ln\frac{\rho_1}{a} + \frac{j\omega\mu_o}{4\pi M} \sec\psi \ln\frac{2}{\pi c} + \frac{Z_w \sec^2\psi}{2M} \tag{81a}$$

$$Z_s = -\frac{j\omega\mu_o}{4\pi M} \sec\psi \ln\frac{2}{\pi c} - \frac{Z_w \sec^2\psi}{2M} \tag{81b}$$

$$Y = j\omega\left[\frac{1}{2\pi\varepsilon_1} \ln\frac{\rho_1}{a} + \frac{\cos\psi}{2\pi M(\varepsilon_1 + \varepsilon_2)} \ln\frac{2}{\pi c}\right]^{-1} \tag{81c}$$

$$\Gamma_s = -\frac{\cos\psi}{2\pi M(\varepsilon_1 + \varepsilon_2)} \ln\frac{2}{\pi c}\,\frac{Y}{j\omega} \tag{81d}$$

This completes the evaluation of the cable parameters for this shield model. We may write Z in the form

$$Z = Z_c - Z_s \tag{82}$$

where

$$Z_c = j\omega L_c = \frac{j\omega\mu_o}{2\pi} \ln \frac{\rho_1}{a} \tag{83}$$

and furthermore Y may be written

$$Y = \frac{j\omega}{S_c - S_s} \tag{84}$$

where

$$S_c = \frac{1}{2\pi\varepsilon_1} \ln \frac{\rho_1}{a} \tag{85a}$$

$$S_s = - \frac{\cos\psi}{2\pi M \ (\varepsilon_1 + \varepsilon_2)} \ln \frac{2}{\pi c} \tag{85b}$$

also

$$\Gamma_s = \frac{S_s}{S_c - S_s} \tag{86}$$

Z_c and S_c are the quantities descriptive of a shield confined to a thin layer around $\rho = \rho_1$; Z_s contains a term due to the "openness" of the shield structure and one due to the finite resistance of the shield wires. S_s includes the effects of the open shield structure and the presence of the dielectric jacket. One will note that Z_s and S_s both decrease as M is made large but c is held constant. This is in agreement with the results obtained by other authors (refs. 2,4), who have indicated that for fixed optical coverage, better shielding is obtained if there are many small holes in the shield than if there are few large ones.

The relative importance of the finite resistance of the braid-shield conductors and the finite optical coverage in contributing to Z_s is easily found. The ratio of the magnitude of the second term in Eq. (81b) to that of the first is given by

$$r_{Z_s} = \left| \frac{2\pi \sec\psi \; Z_w}{j\omega\mu_o \; \ell n \frac{2}{\pi c}} \right| = \frac{\sec\psi}{\ell n \frac{2}{\pi c}} \left| \frac{I_o(\tau_w b)}{\tau_w b \; I_1(\tau_w b)} \right| \tag{87}$$

If the shield wires are highly conductive, then $|\tau_w b| >> 1$, and

$$r_{Z_s} \simeq \frac{\sec\psi}{\ell n \frac{2}{\pi c}} \; \frac{1}{|\tau_w b|} << 1 \tag{88}$$

so that the finite braid resistance makes a far less significant contribution to Z_s than does the finite optical coverage of the shield, as long as ψ is not too large.

Finally, the effect of the dielectric jacket is evident in Eq. (85b). If the jacket is lossy, then $\varepsilon_2 \to -j\infty$ in the low-frequency limit, so that $S_s \to 0$. This physically occurs because the shield layer becomes effectively an equipotential and the effect of the individual shield wires is unimportant insofar as the capacitive coupling is concerned. It will be noted that the thickness of the dielectric jacket does not appear in the expression for S_s. This occurs because S_s is independent of $d = \rho_o - \rho_1$ for most cases of interest (see the Appendix). If $d = 0$, ε_2 should be replaced by ε_o.

SECTION VI

SUMMARY AND DISCUSSION

In this report we have considered the effects of finitely-conducting shields and dielectric weatherproofing jackets on three coaxial-cable models. In the first two models considered, the optical coverage was unity, so that the only field-penetration mechanism through the shield was diffusion of the field through the conducting shield material. Thus the finite resistance of the shield and the imperfect shielding are essentially the same phenomenon: the finite skin depth of the shield. The results obtained for these two models had significant differences in that for the first case, the bidirectionally conducting shell, Z_s decreased exponentially with τd, while in the second case, the two unidirectionally conducting shells, Z_s decreased only algebraically. This difference seems to point up the importance of actually weaving the braid conductors together, as is done in practice. In neither case does the presence of a dielectric jacket have any effect on the shielding, since the capacitive coupling through a shield which is axially and azimuthally uniform is nil.

In the third model considered, the shield was sparse, being made up of filamentary helical conductors with relatively small optical coverage. For this shield, which has a periodic structure around and along its axis, aperture penetration is the dominant field-coupling mechanism and the fact that the wire resistance is not zero is not as important to the coupling as is the low optical coverage. The presence of a dielectric jacket can have a significant effect on the mutual susceptance S_s, inasmuch as S_s is decreased by a factor $(\varepsilon_{r1} + 1)/(\varepsilon_{r1} + \varepsilon_{r2})$ if the jacket is thick. If the jacket is lossy, S_s will vanish in the low-frequency limit and thus eliminate the aperture coupling entirely.

In all cases, the "best" shielding is obtained when the braid angle ψ is as small as possible; when the conductivity of the shield material is as high as possible; and when apertures are present, their total area should be divided as finely as possible.

In this Appendix, we attend to certain mathematical details relevant to the solution of the multifilar helix shield model. It was pointed out in Section V that solutions for any of the unknown coefficients A_{nm} - H_{nm} could be obtained in terms of the current in each filament $\hat{I}_o$, and that these solutions would take the form, e.g., $A_{nm} = M\hat{I}_o A'_{nm}\ \delta_k(n-kM)$, where k is any integer. A'_{nm} - H'_{nm} are thus the coefficients which would be obtained if there were a single helix pair (M=1), with each filament carrying one ampere. It is also evident from Section V that a solution for all the unknown coefficients is not necessary for the problem at hand, A'_{nn} and B'_{nn} being sufficient to yield all the information required to evaluate Z, Z_s, Y, and Γ_s.

If the electromagnetic field components are derived from Ψ and Φ using Eqs. (8), (54)-(59) and the boundary conditions at $\rho = \rho_1$ and $\rho = \rho_o$ imposed using Eqs. (60) and (61) with $\hat{I}_o = 1$, there results the following system of equations in the unknowns A'_{nm} - H'_{nm}:

$$\begin{bmatrix} a_{11} & 0 & a_{13} & a_{14} & 0 & 0 & 0 & 0 \\ a_{21} & a_{22} & a_{23} & a_{24} & a_{25} & a_{26} & 0 & 0 \\ 0 & a_{32} & 0 & 0 & a_{35} & a_{36} & 0 & 0 \\ a_{41} & a_{42} & a_{43} & a_{44} & a_{45} & a_{46} & 0 & 0 \\ 0 & 0 & a_{53} & a_{54} & 0 & 0 & a_{57} & 0 \\ 0 & 0 & a_{63} & a_{64} & a_{65} & a_{66} & a_{67} & a_{68} \\ 0 & 0 & 0 & 0 & a_{75} & a_{76} & 0 & a_{78} \\ 0 & 0 & a_{83} & a_{84} & a_{85} & a_{86} & a_{87} & a_{88} \end{bmatrix} \begin{bmatrix} A'_{nm} \\ B'_{nm} \\ C'_{nm} \\ D'_{nm} \\ E'_{nm} \\ F'_{nm} \\ G'_{nm} \\ H'_{nm} \end{bmatrix} = \begin{bmatrix} 0 \\ 0 \\ b_3 \\ b_4 \\ 0 \\ 0 \\ 0 \\ 0 \end{bmatrix} \qquad (A1)$$

in which

$$a_{11} = -\frac{\lambda_{m1}^2}{j\omega\varepsilon_1} L_1$$

$$a_{13} = \frac{\lambda_{m2}^2}{j\omega\varepsilon_2} I_n(\lambda_{m2}\rho_1)$$

$$a_{14} = \frac{\lambda_{m2}^2}{j\omega\varepsilon_2} K_n(\lambda_{m2}\rho_1)$$

$$a_{21} = \frac{n\beta_m}{j\omega\varepsilon_1\rho_1} L_1$$

$$a_{22} = \lambda_{m1} L_4$$

$$a_{23} = \frac{-n\beta_m}{j\omega\varepsilon_2\rho_1} I_n(\lambda_{m2}\rho_1)$$

$$a_{24} = \frac{-n\beta_m}{j\omega\varepsilon_2\rho_1} K_n(\lambda_{m2}\rho_1)$$

$$a_{25} = -\lambda_{m2} I_n'(\lambda_{m2}\rho_1)$$

$$a_{26} = -\lambda_{m2} K_n'(\lambda_{m2}\rho_1)$$

$$a_{32} = -\frac{\lambda_{m1}^2}{j\omega\mu_o} L_3$$

$$a_{35} = \frac{\lambda_{m2}^2}{j\omega\mu_o} I_n(\lambda_{m2}\rho_1)$$

$$a_{36} = \frac{\lambda_{m2}^2}{j\omega\mu_o} K_n(\lambda_{m2}\rho_1)$$

$$a_{41} = \lambda_{m1} L_2$$

$$a_{42} = \frac{-n\beta_m}{j\omega\mu_o\rho_1} L_3$$

$$a_{43} = -\lambda_{m2} \, I_n'(\lambda_{m2}\rho_1)$$

$$a_{44} = -\lambda_{m2} \, K_n'(\lambda_{m2}\rho_1)$$

$$a_{45} = \frac{n\beta_m}{j\omega\mu_o\rho_1} I_n(\lambda_{m2}\rho_1)$$

$$a_{46} = \frac{n\beta_m}{j\omega\mu_o\rho_1} K_n(\lambda_{m2}\rho_1)$$

$$a_{53} = \frac{\lambda_{m2}^2}{j\omega\varepsilon_2} I_n(\lambda_{m2}\rho_o)$$

(A2)

$$a_{54} = \frac{\lambda_{m2}^2}{j\omega\varepsilon_2} K_n(\lambda_{m2}\rho_o)$$

$$a_{57} = \frac{-\lambda_{mo}^2}{j\omega\varepsilon_o} K_n(\lambda_{mo}\rho_o)$$

$$a_{63} = \frac{-n\beta_m}{j\omega\varepsilon_2\rho_o} I_n(\lambda_{m2}\rho_o)$$

$$a_{64} = \frac{-n\beta_m}{j\omega\varepsilon_2\rho_o} K_n(\lambda_{m2}\rho_o)$$

$$a_{65} = -\lambda_{m2} \, I_n'(\lambda_{m2}\rho_o)$$

$$a_{66} = -\lambda_{m2} \, K_n'(\lambda_{m2}\rho_o)$$

$$a_{67} = \frac{n\beta_m}{j\omega\varepsilon_o\rho_o} K_n(\lambda_{mo}\rho_o)$$

$$a_{68} = \lambda_{mo} \, K_n'(\lambda_{mo}\rho_o)$$

$$a_{75} = -\frac{\lambda_{m2}^2}{j\omega\mu_o} I_n(\lambda_{m2}\rho_o)$$

$$a_{76} = -\frac{\lambda_{m2}^2}{j\omega\mu_o} K_n(\lambda_{m2}\rho_o)$$

$$a_{78} = \frac{\lambda_{mo}^2}{j\omega\mu_o} K_n(\lambda_{mo}\rho_o)$$

$$a_{83} = -\lambda_{m2}\ I_n'(\lambda_{m2}\rho_o)$$

$$a_{84} = -\lambda_{m2}\ K_n'(\lambda_{m2}\rho_o)$$

$$a_{85} = \frac{n\beta_m}{j\omega\mu_o\rho_o} I_n(\lambda_{m2}\rho_o)$$

$$a_{86} = \frac{n\beta_m}{j\omega\mu_o\rho_o} K_n(\lambda_{m2}\rho_o)$$

$$a_{87} = \lambda_{mo}\ K_n'(\lambda_{mo}\rho_o)$$

$$a_{88} = \frac{-n\beta_m}{j\omega\mu_o\rho_o} K_n(\lambda_{mo}\rho_o)$$

$$b_3 = \frac{\sin\psi}{2\pi\rho_1}\ [\delta_k(n-m) - \delta_k(n+m)]$$

$$b_4 = \frac{\cos\psi}{2\pi\rho_1}\ [\delta_k(n-m) + \delta_k(n+m)]$$

where

$$L_1 = I_n(\lambda_{m1}\rho_1)K_n(\lambda_{m1}a) - I_n(\lambda_{m1}a)K_n(\lambda_{m1}\rho_1) \quad \text{(A3a)}$$

$$L_2 = I_n'(\lambda_{m1}\rho_1)K_n(\lambda_{m1}a) - I_n(\lambda_{m1}a)K_n'(\lambda_{m1}\rho_1) \quad \text{(A3b)}$$

$$L_3 = I_n(\lambda_{m1}\rho_1)K_n'(\lambda_{m1}a) - I_n'(\lambda_{m1}a)K_n(\lambda_{m1}\rho_1) \quad \text{(A3c)}$$

$$L_4 = I_n'(\lambda_{m1}\rho_1)K_n'(\lambda_{m1}a) - I_n'(\lambda_{m1}a)K_n'(\lambda_{m1}\rho_1) \quad \text{(A3d)}$$

Equation (A1) is solved for A'_{nm} and B'_{nm} by systematically removing the other unknowns. The procedure used was to solve for C'_{nm} - F'_{nm} in terms of G'_{nm} and H'_{nm}, using the last four equations of (A1); then to solve for G'_{nm} and H'_{nm} in terms of A'_{nm} and B'_{nm} using the third and fourth equations; and finally to solve the first and second equations for A'_{nm} and B'_{nm}. The results are as follows:

$$A'_{nm} = \frac{q_{22}r_1 - q_{12}r_2}{q_{11}q_{22} - q_{12}q_{21}} \tag{A4a}$$

$$\frac{B'_{nm}}{j\omega\mu_o} = \frac{q_{11}r_2 - q_{21}r_1}{q_{11}q_{22} - q_{12}q_{21}} \tag{A4b}$$

in which

$$q_{11} = \frac{-n\beta_m}{k_1^2\rho_1} L_1\Delta + \Gamma_{23}\frac{\lambda_{m1}^2}{k_1^2} L_1\lambda_{mo}\lambda_{m2}\rho_o(\lambda_{m2}K'_{oo}L_5 - \lambda_{mo}K_{oo}L_6)$$

$$- \Gamma_{24}\frac{\lambda_{m1}^2}{k_1^2} L_1\, n\beta_m\, K_{oo}L_5(\varepsilon_{r2} - 1) \tag{A5a}$$

$$q_{12} = \lambda_{m1}L_4\Delta - \Gamma_{23}\lambda_{m1}^2L_3n\beta_mK_{oo}L_5\,\frac{1}{\varepsilon_{r2}}\,(\varepsilon_{r2} - 1)$$

$$- \Gamma_{24}\lambda_{m1}^2\rho_oL_3\,\frac{1}{k_o^2}\,(\lambda_{m2}\lambda_{mo}^2K_{oo}L_6 - \frac{1}{\varepsilon_{r2}}\,\lambda_{mo}\lambda_{m2}^2K'_{oo}L_5) \tag{A5b}$$

$$q_{21} = \lambda_{m1}L_2\Delta + \Gamma_{43}\frac{\lambda_{m1}^2}{k_1^2} L_1\lambda_{mo}\lambda_{m2}\rho_o(\lambda_{m2}K'_{oo}L_5 - \lambda_{mo}K_{oo}L_6)$$

$$- \Gamma_{44}\frac{\lambda_{m1}^2}{k_1^2} L_1\, n\beta_mK_{oo}L_5(\varepsilon_{r2} - 1) \tag{A5c}$$

$$q_{22} = \frac{-n\beta_m}{\rho_1} L_3\Delta - \Gamma_{43}\, n\beta_m K_{oo} L_5 \lambda_{m1}^2 L_3 \frac{1}{\varepsilon_{r2}} (\varepsilon_{r2} - 1)$$

$$- \Gamma_{44}\lambda_{m1}^2 \rho_o L_3 \frac{1}{k_o^2} (\lambda_{m2}\lambda_{mo}^2 K_{oo} L_6 - \frac{1}{\varepsilon_{r2}} \lambda_{mo}\lambda_{m2}^2 K'_{oo} L_5) \tag{A5d}$$

$$r_1 = \Gamma_{23}\, n\beta_m K_{oo} L_5 \frac{b_3}{\varepsilon_{r2}} (\varepsilon_{r2} - 1)$$

$$+ \rho_o \Gamma_{24} \frac{b_3}{k_o^2} (\lambda_{m2}\lambda_{mo}^2 K_{oo} L_6 - \frac{1}{\varepsilon_{r2}} \lambda_{mo}\lambda_{m2}^2 K'_{oo} L_5) \tag{A5e}$$

$$r_2 = \Gamma_{43}\, n\beta_m K_{oo} L_5 \frac{b_3}{\varepsilon_{r2}} (\varepsilon_{r2} - 1)$$

$$+ \rho_o \Gamma_{44} \frac{b_3}{k_o^2} (\lambda_{m2}\lambda_{mo} K_{oo} L_6 - \frac{1}{\varepsilon_{r2}} \lambda_{mo}\lambda_{m2}^2 K'_{oo} L_5) + \Delta b_4 \tag{A5f}$$

with

$$\Gamma_{23} = - \frac{n\beta_m}{\lambda_{m2}^2} \frac{\rho_o}{k_o^2 \rho_1} (\lambda_{m2}\lambda_{mo}^2 K_{oo} L_6 - \frac{1}{\varepsilon_{r2}} \lambda_{mo}\lambda_{m2}^2 K'_{oo} L_5) - \frac{n\beta_m K_{oo} L_7}{\lambda_{m2}} (\varepsilon_{r2} - 1) \tag{A6a}$$

$$\Gamma_{24} = \lambda_{mo}\rho_o(\lambda_{mo} K_{oo} L_8 - \lambda_{m2} K'_{oo} L_7) + \frac{n^2\beta_m^2 K_{oo} L_5}{\lambda_{m2}^2 \rho_1\, \varepsilon_{r2}} (\varepsilon_{r2} - 1) \tag{A6b}$$

$$\Gamma_{43} = \frac{\varepsilon_{r2}\rho_o}{\lambda_{m2}} (\lambda_{m2}\lambda_{mo}^2 K_{oo} L_8 - \frac{1}{\varepsilon_{r2}} \lambda_{mo}\lambda_{m2}^2 K'_{oo} L_7) + \frac{n^2\beta_m^2 K_{oo} L_5}{\lambda_{m2}^2 \rho_1} (\varepsilon_{r2} - 1) \tag{A6c}$$

$$\Gamma_{44} = - \frac{n\beta_m \lambda_{mo}}{\lambda_{m2}} \frac{\rho_o}{\rho_1} (\lambda_{mo} K_{oo} L_6 - \lambda_{m2} K'_{oo} L_5) - \frac{n\beta_m K_{oo} L_7}{\lambda_{m2}} k_o^2 (\varepsilon_{r2} - 1) \tag{A6d}$$

$$\Delta = \lambda_{mo}\lambda_{m2}\frac{\rho_o^2}{k_o^2}(\lambda_{mo}^2\lambda_{m2}K_{oo}L_6 - \frac{1}{\varepsilon_{r2}}\lambda_{mo}\lambda_{m2}^2K'_{oo}L_5)(\lambda_{mo}K_{oo}L_6 - \lambda_{m2}K'_{oo}L_5)$$

$$- \frac{n^2\beta_m^2K_{oo}^2L_5^2}{\varepsilon_{r2}}(\varepsilon_{r2} - 1)^2 \tag{A6e}$$

$$L_5 = I_n(\lambda_{m2}\rho_1)K_n(\lambda_{m2}\rho_o) - I_n(\lambda_{m2}\rho_o)K_n(\lambda_{m2}\rho_1) \tag{A6f}$$

$$L_6 = I_n(\lambda_{m2}\rho_1)K'_n(\lambda_{m2}\rho_o) - I'_n(\lambda_{m2}\rho_o)K_n(\lambda_{m2}\rho_1) \tag{A6g}$$

$$L_7 = I'_n(\lambda_{m2}\rho_1)K_n(\lambda_{m2}\rho_o) - I_n(\lambda_{m2}\rho_o)K'_n(\lambda_{m2}\rho_1) \tag{A6h}$$

$$L_8 = I'_n(\lambda_{m2}\rho_1)K'_n(\lambda_{m2}\rho_o) - I'_n(\lambda_{m2}\rho_o)K'_n(\lambda_{m2}\rho_1) \tag{A6i}$$

$$K_{oo} \equiv K_n(\lambda_{mo}\rho_o) \tag{A6j}$$

$$K'_{oo} \equiv K'_n(\lambda_{mo}\rho_o) \tag{A6k}$$

When $n = 0$, $q_{11} = q_{22} = 0$; and if $m = 0$ as well, $b_3 = 0$ so that $r_1 = 0$. Thus it is evident from Eq. (A4b) that $B'_{oo} = 0$; additionally, $A'_{oo} = r_{200}/q_{2100}$, and in the low-frequency limit, it is easy to show using the small-argument approximations to the modified Bessel functions that

$$A'_{oo} = \frac{1}{\pi}\cos\psi \tag{A7}$$

We shall for the remainder of this Appendix be concerned with the case m=n, $n\neq 0$, in the low-frequency limit. In this limit,

$$\lambda_{no,1,2} \to |\beta_n| \tag{A8}$$

and we find after some manipulation that the low-frequency limiting forms for q_{ij}, r_1, and r_2 are given by

$$q_{11nn} \to \frac{L_1}{k_1^2} n\beta_n^5 \rho_o(\varepsilon_{r2} - 1)K_{oo}^2(L_6L_7 - L_5L_8)$$

$$+ \frac{L_1}{k_1^2} n\beta_n^5 \frac{\rho_o^2}{\rho_1} (\varepsilon_{r2} - \varepsilon_{r1})(K_{oo}L_6 - \frac{1}{\varepsilon_{r2}} K'_{oo}L_5)(K_{oo}L_6 - K'_{oo}L_5) \tag{A9a}$$

$$q_{12nn} \to |\beta_n|^7 \frac{\rho_o^2}{k_o^2} (K_{oo}L_6 - \frac{1}{\varepsilon_{r2}} K'_{oo}L_5)[L_4(K_{oo}L_6 - K'_{oo}L_5)$$

$$- L_3(K_{oo}L_8 - K'_{oo}L_7)] \tag{A9b}$$

$$q_{21nn} \to |\beta_n|^7 \frac{\rho_o^2}{k_o^2} (K_{oo}L_6 - K'_{oo}L_5)[L_2(K_{oo}L_6 - \frac{1}{\varepsilon_{r2}} K'_{oo}L_5)$$

$$- \frac{\varepsilon_{r2}}{\varepsilon_{r1}} L_1(K_{oo}L_8 - \frac{1}{\varepsilon_{r2}} K'_{oo}L_7)] \tag{A9c}$$

$$q_{22nn} \to L_3 n\beta_n^5 \rho_o(\varepsilon_{r2} - 1)K_{oo}^2(L_6L_7 - L_5L_8)$$

$$+ L_3 n\beta_n^5 \frac{\rho_o^2}{\rho_1} (\varepsilon_{r2} - \varepsilon_{r1})(K_{oo}L_6 - \frac{1}{\varepsilon_{r2}} K'_{oo}L_5)(K_{oo}L_6 - K'_{oo}L_5) \tag{A9d}$$

$$r_{1nn} \to \frac{\sin\psi}{2\pi\rho_1} \frac{\rho_o^2}{k_o^2} |\beta_n|^5 (K_{oo}L_6 - \frac{1}{\varepsilon_{r2}} K'_{oo}L_5)(K_{oo}L_8 - K'_{oo}L_7) \tag{A9e}$$

$$r_{2nn} \to \frac{\cos\psi}{2\pi\rho_1} \frac{\rho_o^2}{k_o^2} \beta_o\beta_n^5 (K_{oo}L_6 - \frac{1}{\varepsilon_{r2}} K'_{oo}L_5)(K_{oo}L_6 - K'_{oo}L_5) \tag{A9f}$$

Thus in the low-frequency limit,

$$A'_{nn} \to \frac{\beta_o \cos\psi}{2\pi\rho_1\beta_n|\beta_n|} (K_{oo}L_6 - \frac{1}{\varepsilon_{r2}} K'_{oo}L_5)[L_2(K_{oo}L_6 - \frac{1}{\varepsilon_{r2}} K'_{oo}L_5)$$

$$- \frac{\varepsilon_{r2}}{\varepsilon_{r1}} L_1(K_{oo}L_8 - \frac{1}{\varepsilon_{r2}} K'_{oo}L_7)]^{-1} \tag{A10a}$$

$$\frac{B'_{nn}}{j\omega\mu_o} \to \frac{\sin\psi}{2\pi|\beta_n|} \frac{K'_n(|\beta_n|\rho_1)}{K'_n(|\beta_n|a)} \tag{A10b}$$

where the last result has been simplified by using the definitions of L_j. Furthermore, in this limit,

$$\beta_n \to \frac{2n\pi}{p} = \frac{n}{\rho_1} \tan\psi \tag{A11}$$

We are now in a position to consider the two functions F(0) and G(0). It is clear from Eq. (A10a) and the equation defining $F(\beta_o)$, Eq. (70), that the A'_{nn} terms do not enter into F(0), and thus

$$F(0) = -\frac{\sin^2\psi}{\pi} \sum_{\substack{k=1 \\ n=kM}}^{\infty} L_{4nn}^{(-)} \frac{K'_n(n \tan\psi)}{K'_n(n \frac{a}{\rho_1} \tan\psi)} \tag{A12}$$

Furthermore, from Eqs. (A10a) and (73), we have

$$G(0) = \frac{\csc\psi \cos^2\psi}{\pi} \sum_{\substack{k=1 \\ n=kM}}^{\infty} \frac{1}{n} L_{1nn}^{(-)} (K_{oo}L_6 - \frac{1}{\varepsilon_{r2}} K'_{oo}L_5)$$

$$\cdot [L_2(K_{oo}L_6 - \frac{1}{\varepsilon_{r2}} K'_{oo}L_5) - \frac{\varepsilon_{r2}}{\varepsilon_{r1}} L_1(K_{oo}L_8 - \frac{1}{\varepsilon_{r2}} K'_{oo}L_7)]^{-1} \tag{A13}$$

In Eqs. (A12) and (A13), we have used the facts that the summands are even functions of n. One will also note that F(0) does not involve either ε_{r2} or ρ_o, and so is characteristic only of the helical shield; on the other hand, G(0) depends on the shield structure and on the dielectric jacket surrounding the shield. If the dielectric jacket is absent, G(0) becomes

$$G(0) = \frac{\cos\psi}{\pi} \sum_{\substack{k=1 \\ n=kM}}^{\infty} L_{1nn}^{(-)} \frac{K_n(n \tan\psi)}{K_n(n \frac{a}{\rho_1} \tan\psi)} \tag{A14}$$

In order to simplify the evaluation of F(0) and G(0) we shall assume that M is sufficiently large that the modified Bessel functions may be replaced by their uniform asymptotic forms [5]. Introducing these approximations in Eqs. (A12) and (A13), we obtain after a little algebra

$$F(0) = \frac{\cos\psi}{\pi M} \sum_{k=1}^{\infty} \frac{1}{k} e^{-kMQ} \sinh kMQ^{-} \tag{A15}$$

$$G(0) = \frac{\cos^2\psi}{\pi M} \sum_{k=1}^{\infty} \frac{1}{k} \frac{\varepsilon_{r1} \sinh kMQ^{-} (\cosh kMq + \frac{1}{\varepsilon_{r2}} \sinh kMq)}{[\varepsilon_{r1} \cosh kMQ(\cosh kMq + \frac{1}{\varepsilon_{r2}} \sinh kMq) + \varepsilon_{r2} \sinh kMQ(\sinh kMq + \frac{1}{\varepsilon_{r2}} \cosh kMq)]} \tag{A16}$$

in which

$$Q = \xi(a/\rho_1, \psi) \tag{A17a}$$

$$Q^{-} = Q - \frac{\pi c}{2M} \tag{A17b}$$

$$q = \xi(\rho_0/\rho_1, \psi) \tag{A17c}$$

$$\xi(z,\psi) = |\eta(\tan\psi) - \eta(z\tan\psi)| \tag{A17d}$$

and

$$\eta(x) = \sqrt{1 + x^2} + \ln \frac{x}{1 + \sqrt{1 + x^2}} . \tag{A18}$$

The optical coverage c is given by

$$c = \frac{2Mb}{\pi\rho_1} \sec\psi \leq 1 \tag{A19}$$

It is easy to show that

$$\xi(z,\psi) \geq \xi(z,0) = |\ln z| \tag{A20}$$

and as a consequence

$$2MQ \geq 2M \ln \frac{\rho_1}{a} \tag{A21a}$$

$$2MQ^- \geq 2M \ln \frac{\rho_1}{a} - \pi c \tag{A21b}$$

$$2Mq \geq 2M \ln \frac{\rho_o}{\rho_1} \tag{A21c}$$

Now in typical coaxial cables $\ln \frac{\rho_1}{a}$ is of the order of unity, so that if M is large, as we assume, then

$$2MQ >> 1 \tag{A22a}$$

$$2MQ^- >> 1 \tag{A22b}$$

and we readily obtain

$$F(0) = \frac{\cos\psi}{2\pi M} \sum_{k=1}^{\infty} \frac{1}{k} e^{-k\pi c/2}$$

$$= - \frac{\cos\psi}{2\pi M} \ln (1-e^{-\pi c/2}) \tag{A23}$$

$$G(0) = \frac{\cos^2\psi}{\pi M} \left(\frac{\varepsilon_{r1}}{\varepsilon_{r1} + \varepsilon_{r2}}\right) \sum_{k=1}^{\infty} \frac{1}{k} e^{-k\pi c/2} \left[\frac{1 + f\ e^{-2kMq}}{1 - fg\ e^{-2kMq}}\right] \tag{A24}$$

where

$$f = \frac{\varepsilon_{r2} - 1}{\varepsilon_{r2} + 1} \tag{A25a}$$

$$g = \frac{\varepsilon_{r2} - \varepsilon_{r1}}{\varepsilon_{r2} + \varepsilon_{r1}} \tag{A25b}$$

If the dielectric jacket is absent, then $q = 0$ ($\rho_o/\rho_1 = 1$) or $\varepsilon_{r2} = 1$; and $G(0)$ becomes

$$G(0)\Bigg|_{\text{no jacket}} = -\frac{\cos^2\psi}{\pi M}\left(\frac{\varepsilon_{r1}}{1+\varepsilon_{r1}}\right) \ln\left(1-e^{-\pi c/2}\right) \tag{A26}$$

On the other hand, if $2Mq \gg 1$, i.e., if the jacket is thick and M is large,

$$G(0) \approx -\frac{\cos^2\psi}{\pi M}\left(\frac{\varepsilon_{r1}}{\varepsilon_{r1}+\varepsilon_{r2}}\right) \ln\left(1-e^{-\pi c/2}\right) \tag{A27}$$

To examine the behavior of $G(0)$ for moderate values of $2Mq$, we define a function h as follows:

$$h(\varepsilon_{r1}, \varepsilon_{r2}, c, 2Mq) = \frac{-\pi M \sec^2\psi \, G(0)}{\ln\left(1-e^{-\pi c/2}\right)} \tag{A28}$$

so that

$$h(\varepsilon_{r1}, \varepsilon_{r2}, c, o) = \frac{\varepsilon_{r1}}{\varepsilon_{r1}+1} \tag{A29a}$$

$$h(\varepsilon_{r1}, \varepsilon_{r2}, c, \infty) = \frac{\varepsilon_{r1}}{\varepsilon_{r1}+\varepsilon_{r2}} \tag{A29b}$$

A plot of $q = \xi(\rho_o/\rho_1, \psi)$ as a function of ρ_o/ρ_1 for various values of ψ is shown in Fig. A1 and h is plotted as a function of $2Mq$ for various values of ε_{r1}, ε_{r2}, and c in Figs. A2–A7. It is evident in all the cases shown that h has essentially reached its final value for $2Mq > 4$; therefore, for large M, the result for $G(0)$ given in Eq. (A27) may be considered to be accurate whenever $\rho_o/\rho_1 > 1 + 2/M$.

The dependence of h upon the optical coverage c may be seen by comparing Figs. A2 and A5; A3 and A6; and A4 and A7. Increasing c causes h to increase slightly so that its final value is not reached as quickly as 2Mq is increased. This result is reasonable from a physical viewpoint, since an increase in the optical coverage of the shield means that less of the field in the cable interior can penetrate the dielectric jacket. For very small values of c, the final values of h are reached very rapidly as 2Mq is increased.

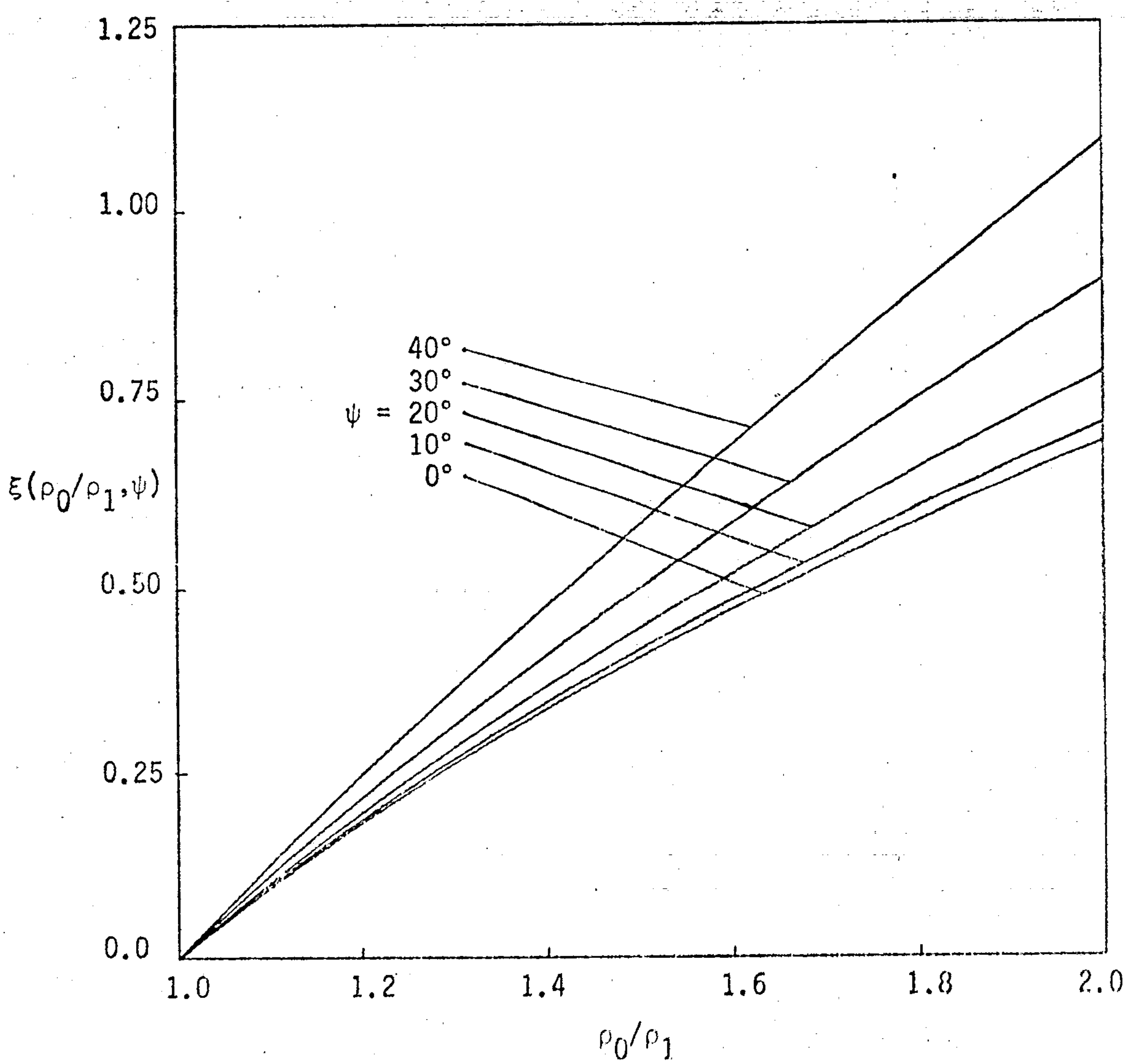

Fig. A1. $\xi(\rho_o/\rho_1, \psi)$ vs. ρ_o/ρ_1 for various values of ψ.

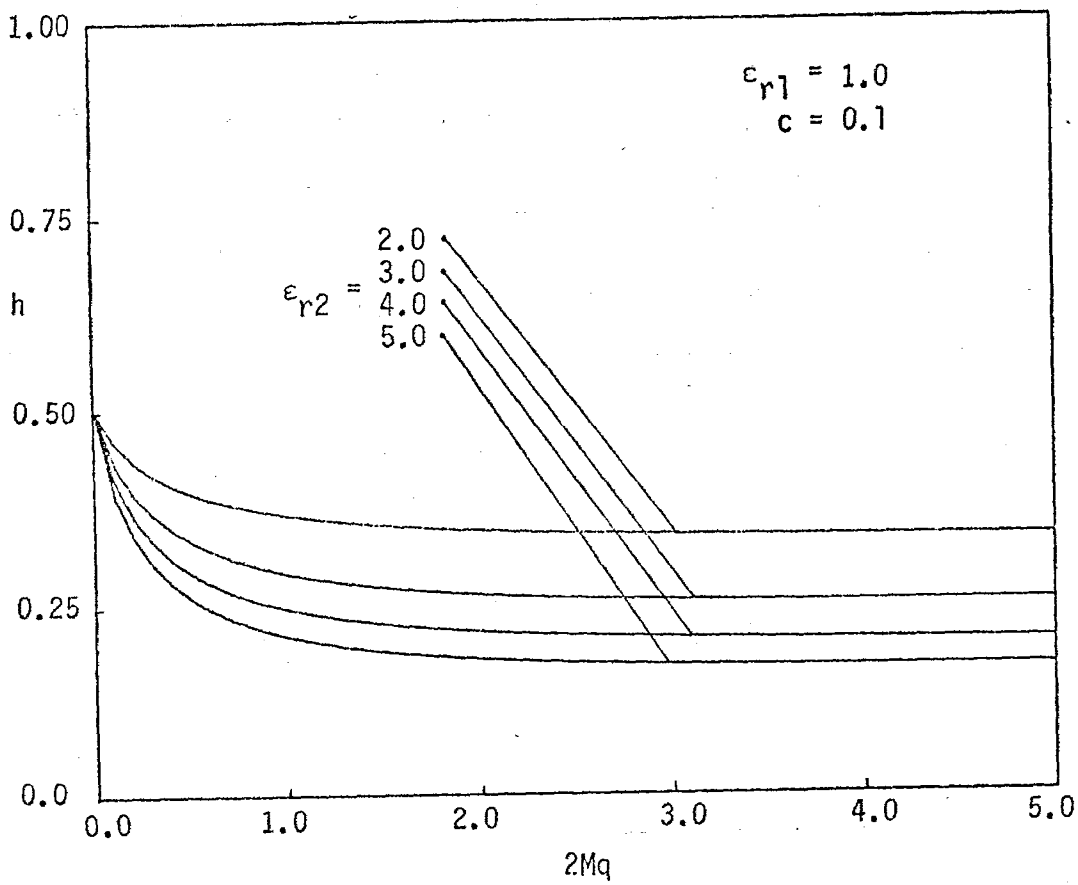

Fig. A2. h vs. 2Mq; $\varepsilon_{r1} = 1$, $c = 0.1$.

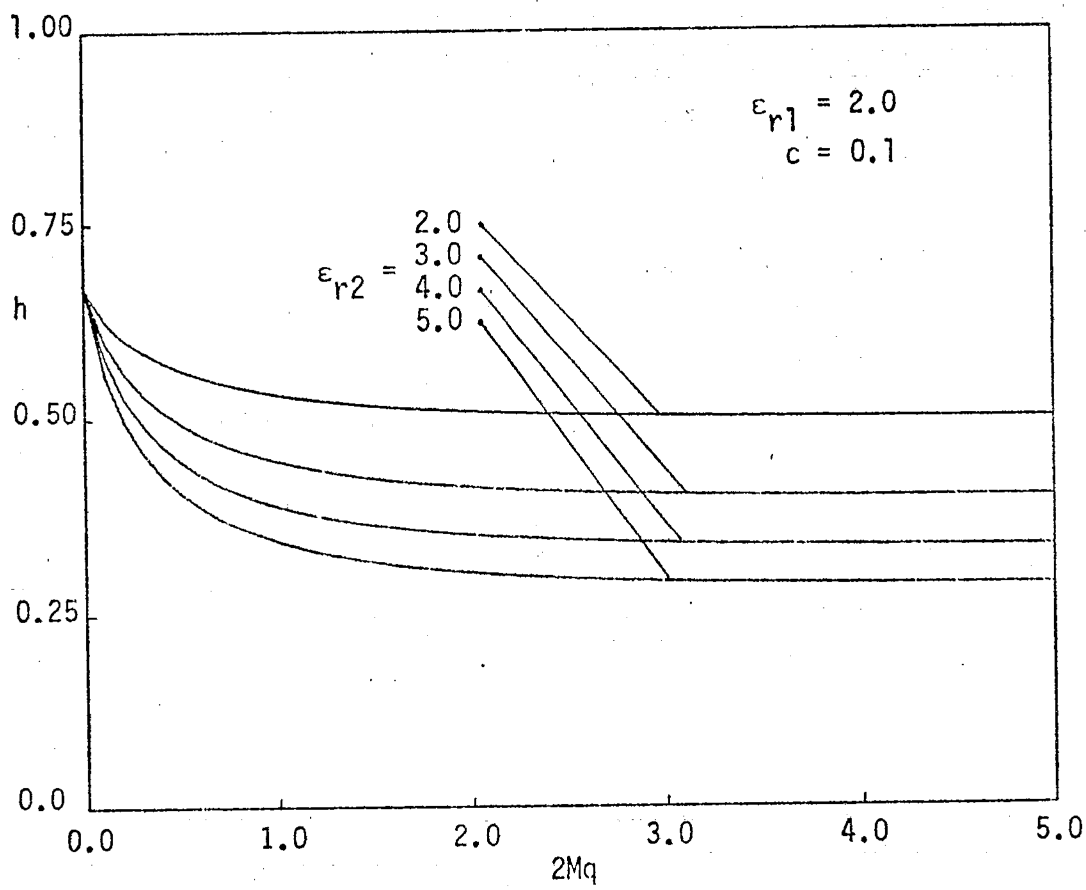

Fig. A3. h vs. 2Mq; $\varepsilon_{r1} = 2$, $c = 0.1$.

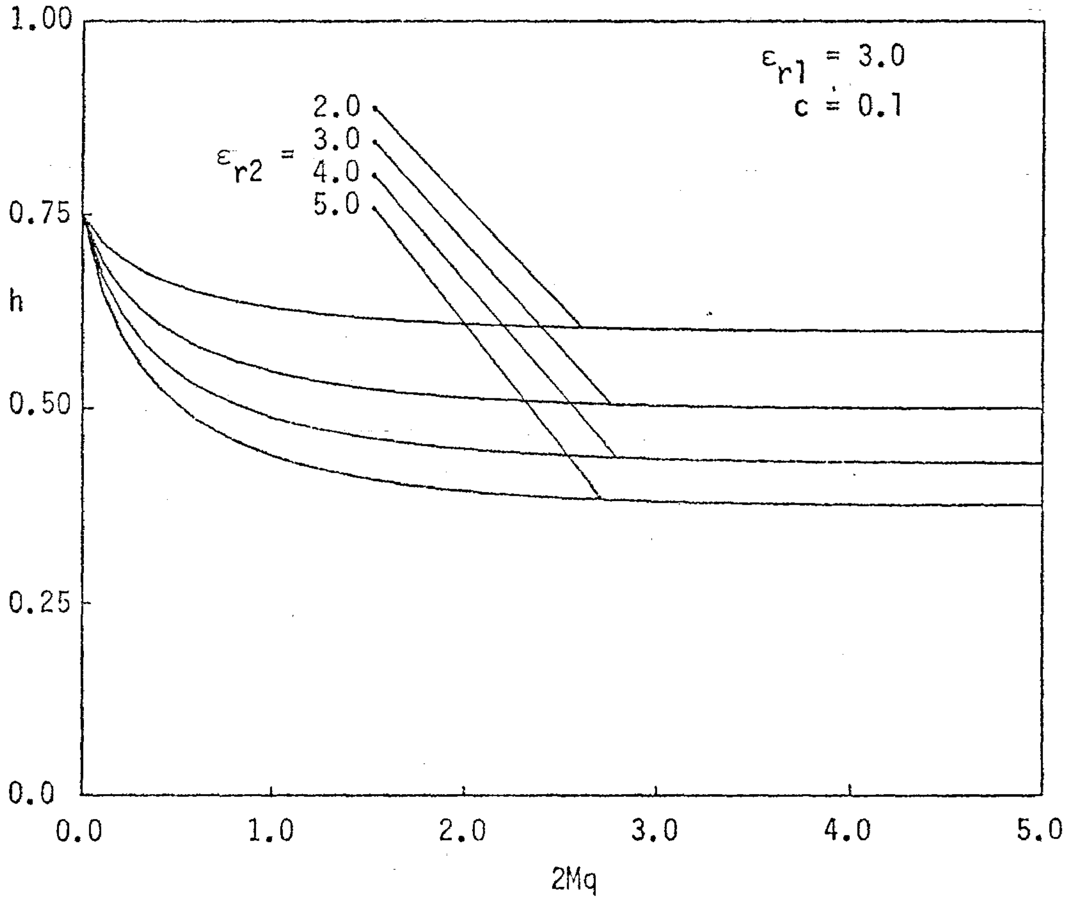

Fig. A4. h vs. 2Mq; $\varepsilon_{r1} = 3$, c = 0.1.

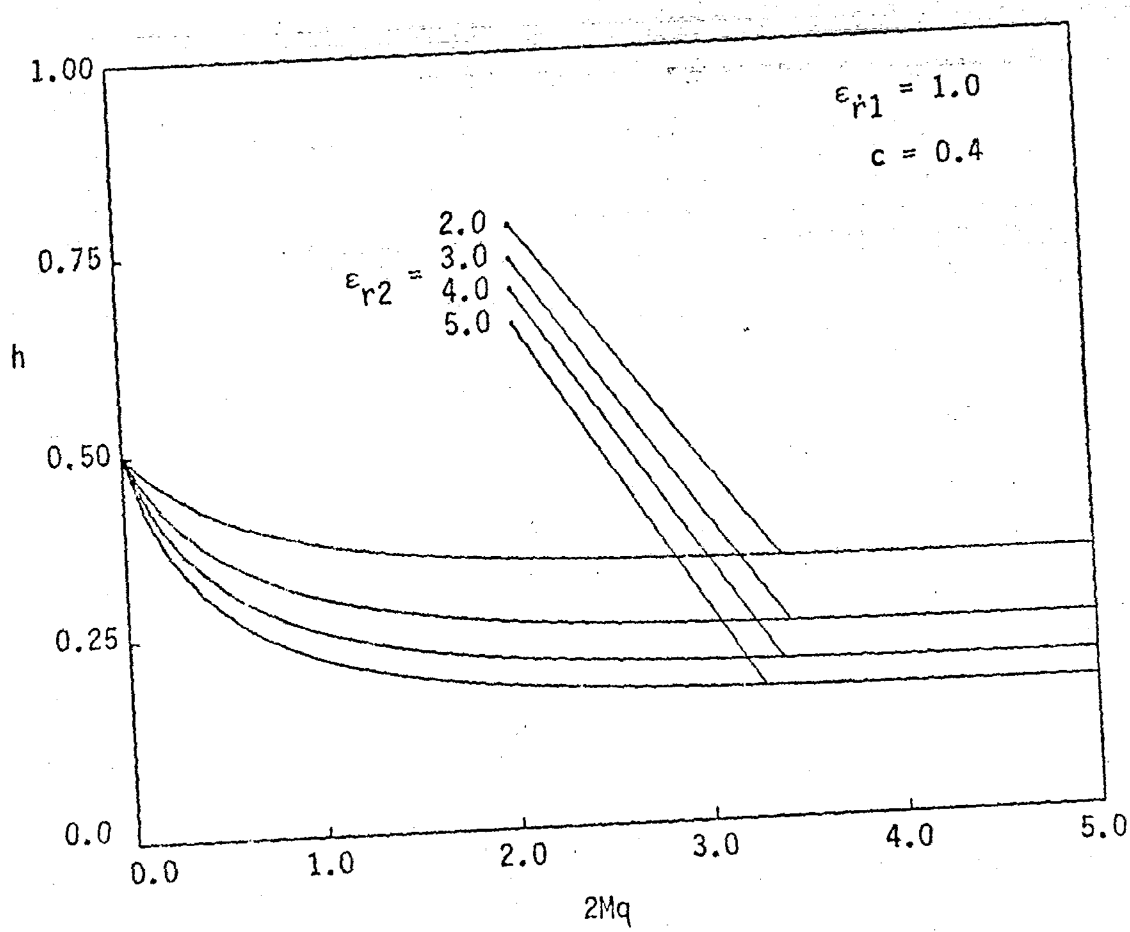

Fig. A5. h vs. 2Mq; $\varepsilon_{r1} = 1$, $c = 0.4$.

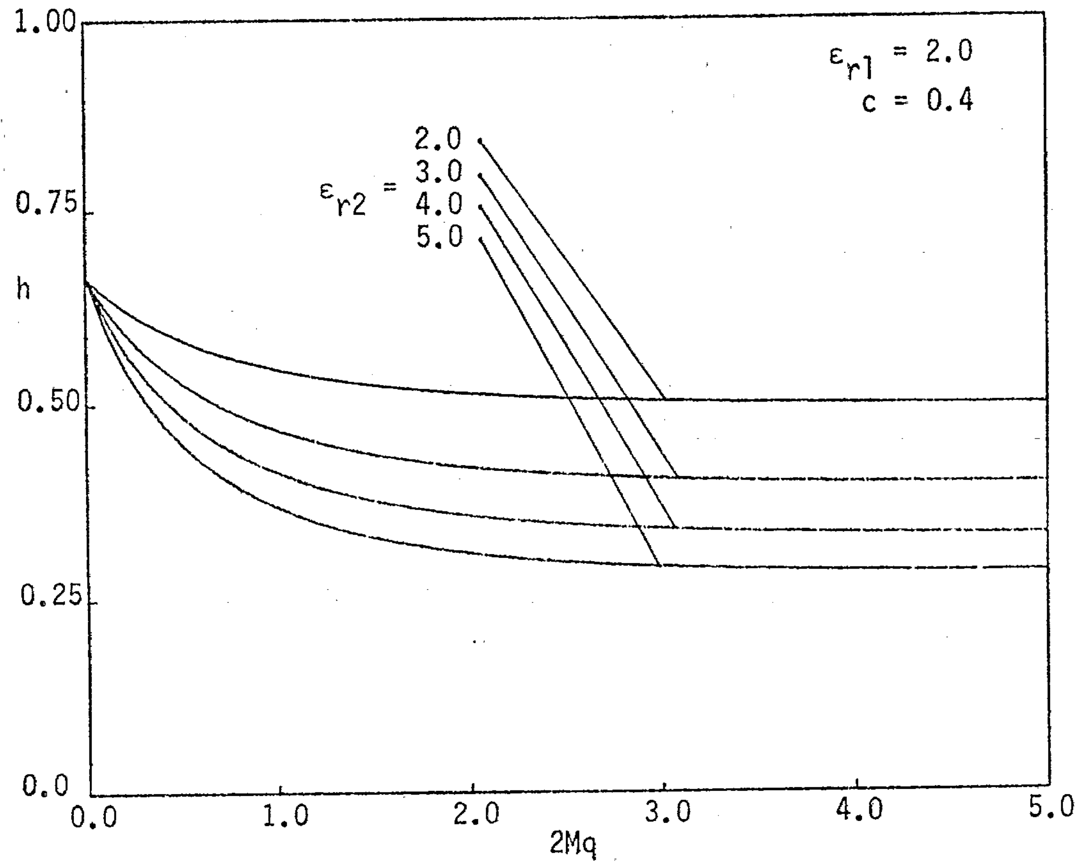

Fig. A6. h vs. 2Mq; ε_{r1} = 2, c = 0.4.

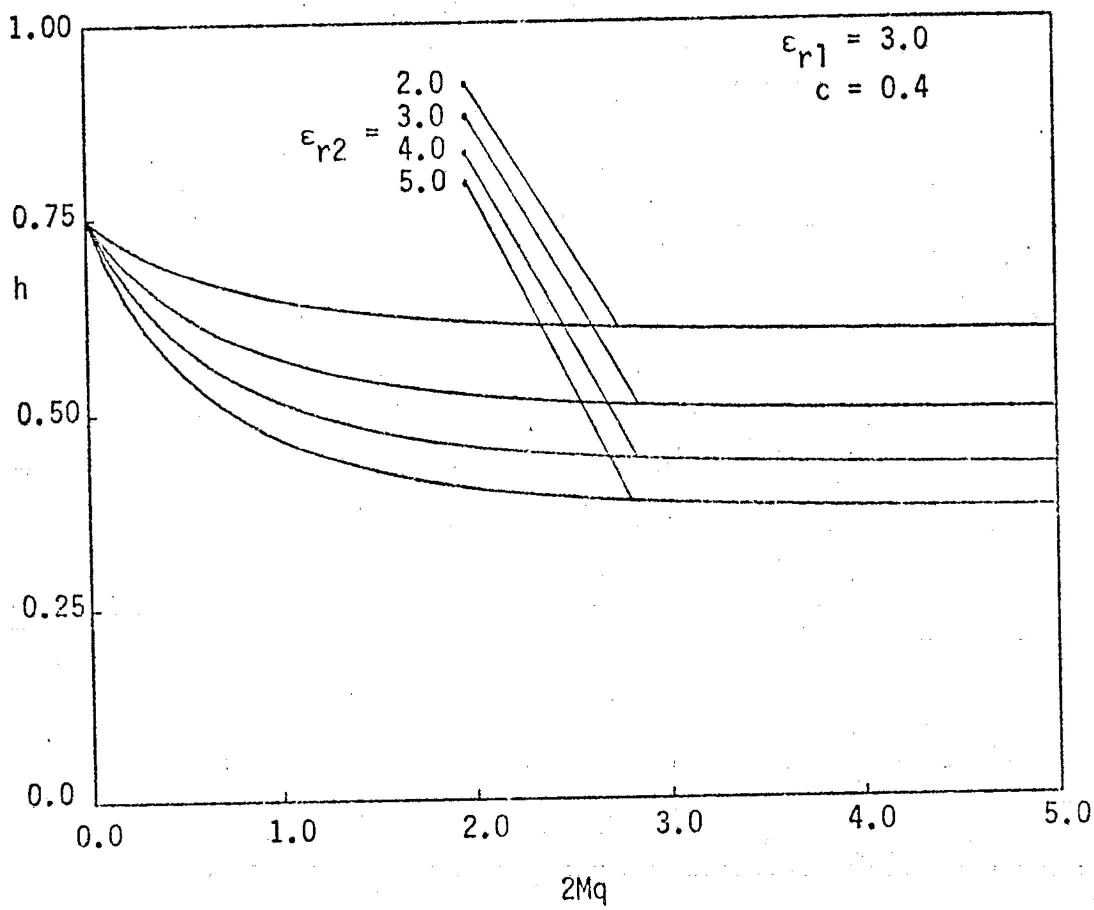

Fig. A7. h vs. 2Mq; $\varepsilon_{r1} = 3$, $c = 0.4$.

REFERENCES

[1] R. W. Latham, "An Approach to Certain Cable Shielding Calculations," Interaction Note 90, January 1972.

[2] E. F. Vance, "Shielding Effectiveness of Braided Wire Shields," Interaction Note 172, April 1974.

[3] K. F. Casey, "Induced Currents on a Cable Shielded by Two Unidirectionally Conducting Shells," Interaction Note 133, May 1973.

[4] K. S. H. Lee and C. E. Baum, "Application of Modal Analysis to Braided-Shield Cables," Interaction Note 132, January 1973.

[5] M. Abramowitz and I. A. Stegun, editors, Handbook of Mathematical Functions, National Bureau of Standards, AMS-55, June 1964, p. 378.

10/25/85